Refined Macroscopic Traffic Modelling Via Systems Of Conservation Laws

by

Ashlin D. Richardson
B.Sc., University of Victoria, 2008

A Thesis Submitted in Partial Fulfillment of the
Requirements for the Degree of

MASTER OF SCIENCE

in the Department of Mathematics and Statistics

Refined Macroscopic Traffic Modelling
Via Systems Of Conservation Laws

by

Ashlin D. Richardson
B.Sc., University of Victoria, 2008

Supervisory Committee

Dr. Reinhard Illner, Supervisor
(Department of Mathematics and Statistics, University of Victoria)

Dr. Martial Agueh, Departmental Member
(Department of Mathematics and Statistics, University of Victoria)

Supervisory Committee

Dr. Reinhard Illner, Supervisor
(Department of Mathematics and Statistics, University of Victoria)

Dr. Martial Agueh, Departmental Member
(Department of Mathematics and Statistics, University of Victoria)

ABSTRACT

We elaborate upon the **Herty-Illner macroscopic traffic models** [1, 2, 3] which include special non-local forces. The first chapter presents these in relation to the traffic models of Aw-Rascle [4] and Zhang [5], arguing that non-local forces are necessary for a realistic description of traffic.

The second chapter considers **travelling wave solutions** for the Herty-Illner macroscopic models. The travelling wave ansatz for the braking scenario reveals a curiously implicit nonlinear **functional differential equation**, the **jam equation**, whose unknown is, at least to conventional [6, 7] tools, inextricably self-argumentative! Observing that analytic solution methods [8] fail for the **jam equation** yet succeed for equations with similar coefficients raises a challenging problem of pure and applied mathematical interest. An **unjam equation** analogous to the **jam equation** explored by Illner and McGregor [9] is derived.

The third chapter outlines **refinements** [3] for the Herty-Illner models [1, 2]. **Numerics** [10, 11, 12] allow exploration of the refined model dynamics in a variety of realistic traffic situations, leading to a discussion of the broadened applicability conferred by the refinements: ultimately the prediction of **stop-and-go waves**.

The conclusion asserts that all of the above contribute knowledge pertinent to traffic control for reduced congestion and ameliorated vehicular flow.

Contents

List of Figures

List of Tables

ACKNOWLEDGEMENTS

First and foremost I express my thanks and deep gratitude to Professor Reinhard Illner for his kindness, support, and patient supervision.

I am grateful to Professor Martial Agueh and Professor Henning Structrup for their support as committee members.

I thank Professor Reinhard Illner and Professor Michael Herty for the opportunity to present their work.

I thank Professor Bruce Gooch for graciously providing the opportunity to finish the thesis while already his PhD student in the Department of Computer Science.

Most of all I thank my family and friends who made this possible.

And if you gaze for long into an abyss, the abyss gazes also into you.
Friedrich Nietzsche

DEDICATION

To Chloë

Chapter 1

Analysis Of Traffic Models

Vehicular traffic flow refers to the spatio-temporal interplay between road networks, traffic control technology, vehicles, and drivers. Traffic flow is studied to enhance road network design, in order to reduce congestion and improve the flow of vehicles. Since the behaviour of individual drivers can trigger traffic jams, driver behaviour is an aspect contributing to the complicated features of traffic phenomena.

An important phenomenon indicated by both theoretical [13] and empirical [14] traffic studies is the existence of a traffic density threshold or bifurcation point above which the flow becomes unstable, whereby minor disturbances result in large moving jams. Drivers react to the braking of those ahead, in turn, triggering others behind to brake. Since this thesis is largely concerned with the elucidation, from macroscopic traffic models, the characteristic profiles of such jams moving along road segments, such braking cascades represent the primary object of interest. Studied in the three chapters are the following: 1) the existence of moving jams 2) the functional equations resulting from the existence question, and finally 3) the numerical existence of oscillations (stop-and-go waves) representative of the concatenation of successive (idealized) braking waves with acceleration waves (such oscillations are both expected and observed).

The existence of travelling wave solutions has been postulated for a number of macroscopic traffic models, possibly giving closed form solution formulae [13]. A highlight of the work of Herty and Illner [1, 2] is an innovative non-local interaction term, well motivated through reasonable modelling assumptions; in contrast the force terms presented by many authors are developed, arguably, in questionably close analogy to fluid mechanics. The novelty of Herty and Illner's force term is the non-locality arising from modelling the reaction of drivers to their observations some

distance ahead. Although the non-locality introduced makes the system harder to solve, they argue that this kind of non-locality is an essential aspect of traffic flow that should not be neglected.

That the non-locality is necessary is Herty and Illner's thesis, which is put forward in the first chapter. Here macroscopic traffic models are introduced with explanation of their relationship with both microscopic [15] and kinetic (mesoscopic) [16] traffic models. The Herty-Illner [1, 2] macroscopic traffic models related to those of Aw-Rascle [4] and Zhang [5] are presented, for which truncation of the system by Taylor-expansion yields an equation of Hamilton-Jacobi type (with diffusion): thus the Herty-Illner macroscopic traffic model generalizes the well known model of Aw-Rascle [4] and Zhang [5]. This simplified model is investigated qualitatively and quantitatively for regimes of accelerating and braking traffic.

The second chapter develops functional equations arising from the application of a travelling wave ansatz to the Herty-Illner [1, 2] macroscopic traffic model. In addition to the braking case considered in [1, 2, 9] the existence of travelling wave solutions is considered for the acceleration case of the macroscopic traffic model. By the travelling wave ansatz, the fully non-local model yields a curiously implicit nonlinear functional differential equation (the *jam equation*) whose unknown function refers to itself as its own argument; thus the unknown is difficult to resolve, at least using the conventional methods for delayed functional differential equations [6, 7] which do not treat the case of functional iteration of the unknown. The observation that analytic solution approaches [8] fail for the *jam equation* while succeeding for equations with almost the same coefficients raises a challenging problem of pure and applied mathematical interest.

The third chapter introduces a refined Herty-Illner macroscopic model [3] and associated numerics adapted by Herty from Leveque [10, 11, 12]. The refinements [3] extend those given to the original model [1] in [2]: the usual non-local term (representative of driver interaction) is augmented and reconciled with a relaxation term (representative of free-flow dynamics). The model refinements and associated numerical experiments demonstrate a realistic description of traffic dynamics which predicts that stop-and-go waves will form.

1.1 Introduction to Traffic Modelling

Three approaches to traffic modelling are prominent in the literature: microscopic, kinetic (mesoscopic), and macroscopic [17, 18, 19]. The importance in bringing attention to each of them is due to their complementarity: for consistency with our experience, a model corresponding to one descriptional stratum should ideally be fully representative of the situations at the other strata. This points to a statement of models that may be outside the usual distinctions between scales.

Microscopic models, the most detailed, evolve the system according to Newton's law, accounting for each car on an individual basis. Typically this is accomplished with a system of differential equations: one equation for each car. The couplings between the equations represent the interactions.

The coarser mesoscopic or kinetic approaches account for groups of cars with the same kinetic parameters: that is, they study the number of cars at a given time, position, and speed, through a distribution function $f(t, x, v)$, which evolves over time according to a kinetic transport equation [20]. Not limited to the description of human behaviour, the kinetic equation framework may provide an avenue for the discussion of the collective behaviour of other species [21].

Macroscopic models, coarser still, do not even track groups of cars, instead modelling the traffic flow as a continuum, by way of macroscopic variables. Macroscopic models typically consider the density of cars $\rho(x, t)$ and speed of cars $u(x, t)$ as a function of time and space; these quantities evolve according to partial differential equations. Here attention is mostly directed to macroscopic models. Next, examples are reviewed to introduce all three model types.

1.1.1 Microscopic Models

The microscopic modelling strategy prescribes the forces acting on the cars, so that the systemic evolution is governed by Newton's law:

$$F = m \cdot \ddot{x}(t)$$

from which successive integrations may be used to derive $\dot{x}(t)$ and $x(t)$. Beyond the usual study via ordinary differential equations, the possible inclusion of a reaction time τ promotes the investigation to the realm of differential delay equations. A number of cars being situated along a one dimensional road, an example of a microscopic traffic

model [15] formulated from Newton's law is

$$\ddot{x}_i(t+\tau) = g\left(\frac{1}{x_{i-1}(t) - x_i(t)}\right)[\dot{x}_{i-1}(t) - \dot{x}_i(t)] \tag{1.1}$$

where the indices i progress from 0 up to $n-1$ to represent n cars (0 is the index of the leading car). According to (1.1) the accelerating force on the car with index i is proportional to the relative speed with respect to the car ahead: $[\dot{x}_{i-1}(t) - \dot{x}_i(t)]$. Therefore a driver attempts to match the speed of the car ahead. Also in (1.1) the assumed dependency of the accelerating force is in direct proportion with some function $g(\cdot)$ of the density $\rho_i(t)$, where the so-called density $\rho_i(t)$ refers directly to the reciprocal of the distance to the car ahead $\frac{1}{x_{i-1}(t)-x_i(t)}$. The function $g(\cdot)$ is chosen so that cars respond to high density (low density) situations with deceleration (acceleration). In the presentation of this model [15] Illner notes that passing or collision events are outside the domain of applicability.

1.1.2 Mesoscopic (Kinetic) Models

Rather than tracking the position and velocity of individual cars, mesoscopic (kinetic) models track the position and velocity of infinitesimal density elements. This is accomplished by a dynamical system which temporally evolves a probability density $f(x, v, t)$ valued in displacement, velocity, and time. Moreover this evolution is typically accomplished using partial differential equation models as used in the dynamics of statistical physics (e.g. Boltzmann and Boltzmann-like equations) in the continuous context. Such probabilistic approaches lead to the consideration of the following interpretations:

- In a traffic model, cars of different velocities might occupy the same space.
- Since the treatment of interactions (for example, lane changing in multi-lane traffic models) is probabilistic, the model effectively tracks (simultaneously) the system's evolution through all possible traffic scenarios.
- Then (as with quantum mechanics) kinetic models often are interpreted by taking statistical moments, for qualitative study of dynamics from the model.
- Such traffic dynamics patterns as represented by statistical moments are representative of aggregated (collective) behaviour of the possible traffic dynamics patterns that the model rules admit.

- Finally, as we shall see, applying a "synchronized traffic" assumption (local similarity of velocities) results in a macroscopic model being derived from a kinetic one.

For illustration a brief overview of the Vlasov-Fokker-Planck traffic model [20], a kinetic traffic model, is provided. This pertains to the macroscopic models to be considered [1, 2] since Herty and Illner derive them [1, 2] from the same type of kinetic model [20]. De temps a temps, Macroscopic models have been (sometimes rightfully) dismissed as mere (poor) analogies with fluid dynamics. Accordingly, the derivation of a macroscopic model from a kinetic one puts the macroscopic model on a first-principles basis that allows direct statistical interpretation demonstrating the sound basis of the macroscopic model in terms of interaction rules between individual cars (the basis of all traffic models). The advantage of the macroscopic approach is the applicability of analytic (continuous) methods to study qualitative traffic behaviour.

Vlasov-Fokker-Planck model for high density traffic

The Vlasov-Fokker-Planck model [20] is a partial differential equation describing traffic dynamics, as represented by the unknown kinetic density function $f_i(t, x, v)$. As the model is applicable to multi-lane traffic flow the $i-$subscript denotes the lane index. The solution of the system is thus, for each lane i, a vehicular density associated with the time t, displacement x, and velocity $v > 0$. For a two lane system ($i \in 1, 2$) the model equation is (where $k = 3 - i$ denotes the index of the other lane):

$$\partial_t f_i + v\partial_x f_i + \partial_v(B[f_i] \cdot f_i - D[f_i] \cdot \partial_v f_i) = p_k[f_k] \cdot f_k - p_i[f_i] \cdot f_i. \qquad (1.2)$$

Aside from the usual transport terms, $\partial_v(B[f_i]f_i - D[f_i]\partial_v f_i)$ represents interactions between cars: $B[f_i]$ is the braking/acceleration force, $D[f_i]$ is an optional diffusion term, and $p_k[f_k] \cdot f_k - p_i[f_i] \cdot f_i$ represents the effects of lane changing. We note that multi-valued fundamental diagrams may be obtained from this model if equilibrium states are assumed.

Although multi-lane traffic models could be studied (in deriving a macroscopic model from the kinetic model there would be, in correspondence with the lanes, a family of systems of equations like (1.20)) we are concerned here single-lane (or lane-homogenized) traffic models. To this end, the single-lane (or lane-homogenized) version of (1.3) is considered:

Vlasov model for single-lane (lane-homogenized) traffic

The Vlasov [1] model for single-lane or lane-homogenized traffic flow is:

$$\partial_t f + v\partial_x f + \partial_v(B(\rho, v - u^X)f) = 0 \tag{1.3}$$

which, relative to the predecessor (1.2), has the following simplifying modifications:

- The $i-$index is lost, since the density refers to single-lane (or lane-homogenized) traffic.
- The diffusion and lane-changing effects are omitted.
- The dependency of $B(\rho, v - u^X)$ will be made specific.

Relative to (1.2), $B(\rho, v-u^X)$ depends on the macroscopic density $\rho(x,t)$ rather than $f(x,v,t)$. The density ρ and relative velocity $v - u^X$ terms upon which $B(\rho, v - u^X)$ depends, we shall elaborate upon imminently. The dependence of $B(\rho, v - u^X)$ upon the macroscopic quantities ρ and u^X is realistic, necessary for consistency, and makes possible the derivation of a macroscopic model (1.20) from the kinetic model.

Derivations of macroscopic models from kinetic models are represented in the literature: in [16] the lane-homogenized version of the kinetic model [20] is used to derive a macroscopic model of Aw-Rascle-Zhang type. In [1, 2] the lane-homogenized version of the kinetic model [20] is used to derive a generalized macroscopic model of Aw-Rascle-Zhang type.

1.1.3 Macroscopic Models

In the conventional interpretation, Macroscopic models do not take account of individual cars but model the flow of cars as a continuum [22]. The popularity of macroscopic models has been hindered somewhat due to a historical tendency to incorrectly develop them in too close of analogy with fluid models: Helbing [23] details these and other criticisms.

The continuous variables involved are termed macroscopic: $\rho = \rho(x,t)$ is the density, $u = u(x,t)$ is the speed. The conventional understanding of these variables is that they are sufficient to describe the traffic system on the grand (macroscopic scale) since they indicate where the cars are, and how fast they are moving. The mass flux, given by $j = j(x,t) = \rho(x,t)u(x,t)$ indicates the quantity of cars moving through an infinitesimal point in unit time.

It is important to discuss in general the interpretation of the macroscopic variables before proceeding to the models, since this interpretation is really what breathes life into them.

Interpreting The Macroscopic Variables

As in [3] when numerically representing macroscopic variables density and speed (ρ and u) might typically be evaluated at intervals representative of stretches of the road corresponding to 20 to 100 meters. Illner [3] notes the propensity for the traffic literature to omit careful discussion of the meaning of ρ and u, a phenomenon leading to substantial misunderstanding among researchers in the traffic community. The usual definition of the macroscopic variables ρ and u with respect to a kinetic (mesoscopic) density $f(x, v, t)$ (valued in space, velocity, and time):

$$\rho(x,t) = \int f(x,v,t)\ dv$$
$$(\rho u)(x,t) = \int v f(x,v,t)\ dv$$

corresponds to (as referred to in the continuum physics community) the **mean field limit** i.e. (in the case of ρ) ρ being the limit as $\Delta x \to 0$ so that $\rho(x)\Delta x$ refers to the particlate quantity within $[x, x + \Delta x]$.

That is, density corresponds to the average number of particles (i.e., cars in the context of traffic modelling) in an interval of length Δx. As Illner indicates [3], this interpretation necessitates that the interval is representative of a large quantity of particles (cars), hence the prescription that ρ and u be studied relative to intervals of magnitude on the order of hundreds of meters (or more); moreover, this interpretation effectively banishes macroscopic models from representation of small-scale features (and dismisses any smaller scale features that might emerge as artifacts).

The alternative interpretation of macroscopic variables ρ, u which Herty and Illner adopt [3] to avoid the last (problematic) interpretation, states that ρ should be interpreted as a (local) estimate of the vehicular density, e.g., modified kernel density estimates, or even modified nearest-neighbor density estimate (i.e., balloon estimates, as they are sometimes referred to in the statistical literature). N.b., the important modification with respect to the usual (statistical) density estimates is the necessity that, in the traffic context, the density estimators be one-sided (corresponding to the propensity for drivers to make decisions predominantly upon conditions ahead).

In particular, Illner suggests $\rho(x_j)$ (the density at position x_j) be taken as the (forward) version of the usual nearest-neighbor density estimate: i.e., assuming individual cars with indices i and positions x_i, $\rho(x_j)$ be taken as the inverse of the distance from the x_j to the nearest car ahead of that at x_j,

$$\rho(x) = \frac{1}{\min\limits_{x \leq x_i}\{x_i - x\}}. \tag{1.4}$$

Of course the analogous expression for u is also possible.

These interpretations of macroscopic (continuum) variables in terms of microscopic variables (the position and velocity of individual cars) as demonstrated in [24] allows the reinterpretation of microscopic models in terms of macroscopic variables, and vice-versa. With this interpretation in hand, the numerical tools available for (nonlinear) hyperbolic systems of equations used to treat the continnum description, may be interpreted as being representative of the microscopic description of traffic dynamics. This is the interpretation that will be assumed throughout.

Such a description is compatible with the idea that all three model types should be mutually intelligible: to highlight the possible interpretations between them we note some derivations in the literature: macroscopic models from microscopic models [24, 25], microscopic models from macroscopic models [26], mesoscopic models from microscopic models [27], and macroscopic models from mesoscopic models [23].

First Order Macroscopic Models

Differential equations of conservation type are typically employed to describe the evolution of continuous variables. In macroscopic traffic models, the mass law is used to relate the evolution of the density $\rho(x,t)$ with the speed $u(x,t)$:

$$\rho_t + j_x = 0.$$

The simple interpretation is that cars are neither created nor destroyed. To close the system a relationship between ρ and u must be prescribed also,

$$j = j(\rho) = \rho u(\rho)$$

from which we interpret $u = u(\rho)$.

Outside of the domain of first order macroscopic models, the more general defini-

tion for flux taken in the kinetic perspective: $j = \rho u(x,t) = \int v f(x,v,t)\, dv$ does not depend solely on ρ but more generally upon v and f.

In the case of first order macroscopic models, the assumed dependency $u = u(\rho)$ implicated by $j = \rho u(\rho)$ is called the fundamental diagram, a relationship which is usually investigated empirically (some examples of fundamental diagrams are given later (3.11,3.12,3.13)). This dependency represents the (limiting) assumption that drivers at a given density are driving at one and only one speed. Combining this assumed dependency with the mass law results in a scalar conservation law, which we call a macroscopic model of first order. The Lighthill-Whitham-Richards (LWR) model:

$$\partial_t \rho + \partial_x(\rho u(\rho)) = 0$$

is the prototype of this family of models [28, 29] where here, $u(\rho)$ is the **preferred velocity** which is usually taken to be a decreasing function of ρ positive for $0 < \rho < \rho_{max}$ (where ρ_{max} a positive maximal density). Since it was defined that $j(\rho) = \rho u(\rho)$ we may also rewrite the above in a form with respect to j:

$$\partial_t \rho + j'(\rho)\partial_x(\rho) = 0. \tag{1.5}$$

A consequence of the first-order treatment (solved by the method of characteristics) is the lack of description of the behaviour near shock waves (where the characteristic lines converge): this is a principal motivation for the development of the second-order models which introduce the second order relationship (analogous to the momentum conservation and/or momentum transfer relationship that is commonplace to the study of fluid, gas, and other dynamics of the transportation of matter). Consequently the second-order relationship prescribes solution behaviour that is meaningful for shocks/discontinuities.

Second Order Macroscopic Models

Alternate to the assumption of the fundamental diagram relationship to close the system, speed may be considered another independent variable, in which case another equation is required for the system to be determined.

Furthermore, the assumed relationship $\rho u = j(\rho) = \rho u(\rho)$ is overly simplistic, since it fails to provide the unstable bifurcative (switching) behaviour that is needed to produce oscillatory behaviour, particularly the destructive stop-and-go oscillations

which are a key feature of congestion.

Accordingly a system of two "conservation equations"[1] may be studied including a law for momentum transfer (in addition to the usual mass law). Aw and Rascle [4] based such a model upon a (momentum) equation of the form:

$$u_t + uu_x - \rho\partial_\rho p(\rho)u_x = 0. \tag{1.6}$$

This model was developed independently by Zhang [5]. The model was studied in the context of a "pressure"[2] law of the form $p(\rho) = c\rho^\gamma$. The Payne-Whitham model [13, 30]:

$$\partial_t u + u\partial_x u + \rho^{-1}p'(\rho)\partial_x\rho = (\tau^{-1})(V(\rho) - u) + u{\partial_x}^2 u \tag{1.7}$$

typically combined with a "pressure" law p such as an isothermal law $p = p(\rho) = \rho$, is historically the first prototype of the second order family of models. In (1.7) the term $V(\rho)$ represents a "preferred speed" or "fundamental diagram" and τ a reaction time, so that, in the linear instantaneous forecast for a given point, the "preferred speed" will be attained τ time-units in the future.

Resurrection of Second Order Traffic Models

Despite a long history of second order "defective" models, Daganzo's "requiem" [31] for them may have been premature. The defects Daganzo observed were inconsistencies related to neglect of crucial distinctions between gas flow and traffic flow: for example the isotropic response of fluid particles to stimuli as opposed to the response of vehicular traffic (this should be more anisotropically predisposed to stimuli ahead).

The model introduced not long after by Aw and Rascle [4] and independently by Zhang [5] served to resolve the inconsistencies that Daganzo documented. Thus the Aw-Rascle-Zhang model brought revived interest towards second-order macroscopic traffic modelling.

We see later that a model closely related to that of Aw-Rascle-Zhang emerges from the Herty-Illner model as an approximation. For now, we examine some basic

[1]The equations are of "conservation type" but are not properly "conservation laws", because the force terms, e.g., the right hand side of $u_t + uu_x = \rho\partial_\rho p(\rho)u_x$, are designed to represent traffic dynamics. Such force terms do not (and should not) conserve momentum.

[2]The term "pressure law" derives from the study of gas dynamics, in which momentum is in fact conserved (in such a case, the term "pressure law" would correspond to the description of an idealized "pressure" force). For (1.6) the term "pressure law" does not really refer to a "pressure" at all, because, although the traffic model is a system of two equations of "conservation type" in which mass conserved, momentum is not conserved (due to the force term).

properties of the Aw-Rascle-Zhang model, namely: the proposition (1.1.5) relates the Aw-Rascle-Zhang model equation (1.6) to a form compatible with the statement of the Herty-Illner macroscopic model (1.20); the proposition (1.1.6) establishes the Aw-Rascle-Zhang model within the context of hyperbolic partial differential equations, and the associated numerical methods.

1.1.4 Intro to Aw-Rascle model

The Aw-Rascle model is of the form:

$$\rho_t + (\rho u)_x = 0 \tag{1.8}$$

$$\rho(u_t + uu_x - \rho\partial_\rho p(\rho)u_x) = 0 \tag{1.9}$$

The following proposition indicates that this system will be represented in the so-called conservation form. The equation (1.6) complementary to (1.9) reflects the practical assumption that $\rho \geq 0$.

1.1.5 Proposition: Equivalent Momentum Law

Assuming $\rho \geq 0$ and the conservation of mass law, (1.6) is equivalent to (1.10):

$$(u + p(\rho))_t + u(u + p(\rho))_x = 0. \tag{1.10}$$

Demonstration. Evidently,

$$\iff u_t + \partial_\rho p(\rho)\rho_t + uu_x + u\partial_\rho p(\rho)\rho_x = 0$$

and since $\rho_t = -\rho u_x = -(\rho)_x u - \rho u_x$ we have:

$$\begin{aligned}
\iff & u_t - \partial_\rho p(\rho)(\rho_x u + \rho u_x) + uu_x + u\partial_\rho p(\rho)\rho_x = 0 \\
\iff & u_t - \partial_\rho p(\rho)\rho_x u - \rho\partial_\rho p(\rho)u_x + uu_x + \partial_\rho p(\rho)\rho_x u = 0.
\end{aligned}$$

Canceling, we have the desired form (1.6).

In the analogous equations for gas dynamics momentum is conserved (such a property has no justification for inclusion in a traffic dynamics model). Equation (1.10) along with the conservation of mass law represents a system of equations of conservation

type: according to the momentum transfer equation the so-called conserved quantity is in fact $u + p(\rho)$ rather than momentum.

1.1.6 Proposition: Hyperbolicity

The following system is strictly hyperbolic:

$$\begin{cases} u_t + uu_x - \rho p_\rho u_x & = 0 \\ \rho_t + \rho_x u + \rho u_x & = 0. \end{cases} \tag{1.11}$$

In matrix form the equations (1.11) are:

$$\begin{bmatrix} u_t \\ \rho_t \end{bmatrix} + \begin{bmatrix} u - \rho p_\rho & 0 \\ \rho & u \end{bmatrix} \begin{bmatrix} u_x \\ \rho_x \end{bmatrix} = \begin{bmatrix} 0 \\ 0 \end{bmatrix}. \tag{1.12}$$

Examining the eigenvalues of $\begin{bmatrix} u - \rho p_\rho & 0 \\ \rho & u \end{bmatrix}$ via the characteristic equation:

$$\det\left(\begin{bmatrix} u - \rho p_\rho & 0 \\ \rho & u \end{bmatrix} - \lambda I \right) = 0$$

indicates that $\lambda^2 + (-2u\rho p_\rho)\lambda - u(-u + \rho p_\rho) = 0$ so that:

$$\vec{\lambda} = \begin{bmatrix} u \\ u - \rho p_\rho \end{bmatrix}. \tag{1.13}$$

Assuming that $\rho p_\rho \neq 0$, the roots are real and distinct; thus the matrix has a linearly independent basis of eigenvectors and we say that the system is strictly hyperbolic.

Consequently, the theory of characteristics applies. Thus, disturbances in the Aw-Rascle model must have a finite propagation speed (as long as the density and "pressure" are finite). The numerical methods for systems of (nonlinear) hyperbolic differential equations apply.

Having placed the second-order macroscopic models within the traffic modelling context and discussed the meaning of the associated variables, we proceed to elaborate upon the Herty-Illner traffic models with which we are primarily concerned.

1.2 The Herty-Illner Macroscopic Model

Prerequisite to the introduction of the Herty-Illner macroscopic model is that of the Vlasov (Kinetic) type model from which the macroscopic model is derived. Subsequent to the definition of the Vlasov model, the macroscopic model is derived from it as a weak-solution concept.

1.2.1 The Herty-Illner Vlasov Model

Where x, v, t denote space, velocity, and time, the **Herty-Illner Vlasov model** is:

$$\partial_t f(x,v,t) + v\partial_x f(x,v,t) + \partial_v\big(B\big(\rho(x,t), v - \boldsymbol{u}^X(x,v,t)\big)f(x,v,t)\big) = 0. \tag{1.14}$$

This model describes the statistical evolution of a particulate system (cars) as a probability density $f(x,v,t)$. It is known as a Vlasov or "collision-less" Boltzmann type equation which, unlike that of Boltzmann, omits the term representative of particulate collisions. Furthermore, there is no diffusion. Also, the force term $B(x,v,t)$ is chosen as forward looking: cars at each space-time position (x,v,t) modify their speed according to those ahead. As the authors indicate, the microscopic equations $x'(t) = v$ and $v' = B(\rho, v - u^X)$ for cars interacting with a force $B(\rho, v - u^X)$ are the characteristics of the Herty-Illner Vlasov equation.

1.2.2 Basic Definitions

The **macroscopic density,** the **macroscopic flux,** and the **non-local average velocity** at $x + H + Tv$ at time $t - \tau$, respectively, are defined as follows:

$$\rho(x,t) = \int f(x,v,t)\ dv \tag{1.15}$$

$$(\rho u)(x,t) = \int v f(x,v,t)\ dv \tag{1.16}$$

$$\boldsymbol{u}^X(x,v,t) = u(x + H + Tv, t - \tau). \tag{1.17}$$

The definition of $\boldsymbol{u}^X$ is intended to reflect that, in the traffic situation, drivers should modify their speed according to that of drivers ahead. The (forward) observational distance $H + Tv$ is taken to reflect a fixed minimum following distance kept by drivers (H), as well as a temporal factor (T) multiplying the driver's speed (e.g., the "two-

second rule"). Finally, the speed observed should be delayed, taking into account the effect of a reaction time (τ) experienced by the driver. In specifying the force term $B()$, the authors note that other choices are possible, but focus on the case:

$$B(\rho, v - u^X) = \begin{cases} -g_1(\rho)(v - u^X) & \text{if } v > u^X \\ -g_2(\rho)(v - u^X) & \text{if } v < u^X \end{cases} \tag{1.18}$$

The form (1.18) is a model for driver behaviour discriminating between scenarios representative of braking ($v > u^X$) and acceleration ($v < u^X$), respectively. In each case, the force applied by the driver is taken to be proportional to the relative velocity $v - u^X$. Furthermore, in each case, the force applied by the driver is taken to depend upon a product of $v - u^X$ with some density dependent factor: $g_1(\rho)$ for braking and $g_2(\rho)$ for acceleration. Possible choices for $g_1(\rho)$ and $g_2(\rho)$ will be discussed later (1.2.4), along with more substantial motivation for (1.18).

Finally we reproduce the definition and derivation [9] of the **Herty-Illner macroscopic traffic model** as a weak solution of the Vlasov model (1.14).

1.2.3 The Herty-Illner Macroscopic Model

Definition: A function f is a **weak solution** of (1.14) if for all smooth $\phi(x, v, t)$ compactly supported in the spatial and temporal variables, and bounded with respect to the velocity, the following holds:

$$T_f(\phi) := \int\int\int [\ \phi_t f + \phi_x v f + \phi_v B(\rho, v - u^X) f]\ dx\, dv\, dt = 0. \tag{1.19}$$

All such ϕ are known as **test functions** for the model. The weak solution concept allows a discussion of generalized solutions that satisfy the partial differential equation (in the sense above) without these solutions necessarily being differentiable.

Proposition: The distributional solution $\rho(x,t)\delta(v - u(x,t))$ is a weak solution of (1.14) in the above sense (1.19) if and only if, almost everywhere:

$$\begin{aligned} \rho_t + (\rho u)_x &= 0 \\ \rho\big(u_t + u_x u - B(\rho, u - u^X)\big) &= 0. \end{aligned} \tag{1.20}$$

The solution ansatz $\rho(x,t)\delta(v-u(x,t))$ is referred to in the literature as the "synchronized traffic" assumption, in which the role of the delta function $\delta(v-u(x,t))$ is to enforce that v and $u(x,t)$ agree. In the context of the "single lane" interpretation of the kinetic model, the interpretation of the assumption is that "locally", speed variations about a point are "small". In the context of the "lane-homogenized" interpretation of the kinetic model, there is the additional interpretation that, at a given point, cars in different lanes travel at the same speed.

Proof: The idea is to use the independence of v with respect to the other variables. We adopt the notation $\partial_i\phi(\xi_1,\xi_2,\xi_3) = \frac{\partial}{\partial\xi_i}\phi(\xi_1,\xi_2,\xi_3)$ and assume a distributional solution that may literally be interpreted as associating a unique velocity $u(x,t)$ with each point (x,t) in space-time:

$$f(x,v,t) = \rho(x,t)\delta(v-u(x,t)). \tag{1.21}$$

This distribution has the special properties (by definition of ρ, δ, u, and v) of: vanishing for x of infinite magnitude, and vanishing also for infinite or negative velocities. Thus it is evident that (1.19) may equivalently be written as:

$$\begin{aligned} T_f(\phi) = \int\int \big[\partial_3\phi\big(x,u(x,t),t\big)\rho(x,t) + \partial_1\phi\big(x,u(x,t),t\big)u(x,t)\rho(x,t) \qquad (1.22)\\ +\partial_2\phi\big(x,u(x,t),t\big)\rho(x,t)B\big(\rho(x,t),u(x,t)-u(x+H+Tu(x,t),t)\big)\big]dx\ dt = 0. \end{aligned}$$

Let us restrict our discussion to ϕ of the form $\phi(x,v,t) = \varphi(x,t)h(v)$ where $v \geq 0$, and make the following definition:

$$\psi(x,t) = \phi(x,u(x,t),t) = \varphi(x,t)h(u(x,t)). \tag{1.23}$$

From the total derivative relationships for ψ (1.23):

$$\psi_t() = \partial_3\phi() + \partial_2\phi()\cdot u_t \tag{1.24}$$

$$\psi_x() = \partial_1\phi() + \partial_2\phi()\cdot u_x \tag{1.25}$$

and the respective definitions for ϕ and ψ above, we list the identities:

$$\partial_3\phi() = \psi_t() - \partial_2\phi() \cdot u_t \tag{1.26}$$

$$\partial_1\phi() = \psi_x() - \partial_2\phi() \cdot u_x \tag{1.27}$$

$$\partial_v\phi = \varphi \cdot h'(v) \tag{1.28}$$

$$\psi(x,t) = \varphi(x,t) \cdot h(u(x,t)). \tag{1.29}$$

Hence if $h(u(x,t)) \neq 0$, $\varphi(x,t) = \frac{\psi(x,t)}{h(u(x,t))}$. We rewrite (1.22) according to (1.26-1.27):

$$\begin{aligned} T_f(\phi) = \int\int \big[&\partial_2\phi\big(x,u(x,t),t\big)\rho(x,t)B(\dots) \\ &+\partial_t\psi(x,t)\rho(x,t) - \partial_2\phi\big(x,u(x,t),t\big)u_t(x,t)\rho(x,t) \\ &+\partial_x\psi(x,t)\rho(x,t)u(x,t) - \partial_2\phi\big(x,u(x,t),t\big)u_x(x,t)u(x,t)\rho(x,t)\big]\ dx\ dt \\ = \int\int &[\partial_t\psi\rho - \partial_2\phi u_t\rho + \partial_x\psi\rho u - \partial_2\phi u_x u\rho + \partial_2\phi\rho B(\dots)]\ dx\ dt = 0. \end{aligned}$$

This representation lends itself to being grouped according to the end result (1.20):

$$\begin{aligned} T_f(\phi) &= \int\int [\partial_t\psi\rho + \partial_x\psi\rho u - \partial_2\phi u_t\rho - \partial_2\phi u_x u\rho + \partial_2\phi\rho B(\dots)]\ dx\ dt \\ &= \int\int [\partial_t\psi\rho + \partial_x\psi(\rho u) - \partial_2\phi(u_t\rho + u_x u\rho - \rho B(\dots))]\ dx\ dt = 0. \end{aligned}$$

Denoting $I = \partial_t\psi\rho + \partial_x\psi(\rho u)$ and $II = \partial_2\phi(u_t\rho + u_x u\rho - \rho B(\dots))$, this is:

$$\int\int I\ dx\ dt\ = \int\int II\ dx\ dt. \tag{1.30}$$

Applying $\varphi(x,t) = \frac{\psi(x,t)}{h(u(x,t))}$ and (1.28) we write II as:

$$\begin{aligned} &\varphi\cdot h'(u(x,t))\big(u_t\rho + u_x u\rho - \rho B(\dots)\big) \\ &= \frac{\psi}{h(u(x,t))}\cdot h'(u(x,t))\big(u_t\rho + u_x u\rho - \rho B(\dots)\big). \end{aligned}$$

Apart from the provisions that $h \neq 0$ and also that φ be compactly supported in both space and time variables we have that $\psi(x,t)$ and $h(u(x,t))$ are arbitrary, whereby $\varphi(x,t) = \frac{\psi(x,t)}{h(u(x,t))}$.That is, the assumptions permit the decomposition of ϕ in terms of independent arbitrary components in space-time (ψ) and velocity (h).

Supposing that the pair of integrals are identically non-zero, due to the independence of ψ and h, $h(s)$ by $\tilde{h}(s) = h^2(s)$, a similar expression to (1.30) where the $\frac{h'(s)}{h(s)}$ in II is replaced by $\frac{\tilde{h}'(s)}{\tilde{h}(s)} = \frac{2h(s)h'(s)}{h(s)^2} = 2\frac{h'}{h}$ is also true. Therefore $\int\int I\ dx\ dt\ = 2\int\int II\ dx\ dt$ necessitating that indeed $\int\int I\ dx\ dt\ = \int\int II\ dx\ dt\ = 0$, whereby the Fundamental Lemma Of Calculus Of Variations permits the conclusion (1.20). On the other hand, supposing (1.20), the equivalent formulation of (1.19) follows immediately:

$$T_f(\phi) = \int\int [\partial_t\psi\rho + \partial_x\psi(\rho u) - \partial_2\phi(u_t\rho + u_x u\rho - \rho B(\dots))]\ dx\ dt = 0$$

by the law of integration by parts. □

Definition: The **Herty-Illner macroscopic model** is the system (1.20).

Before substantially discussing the force terms in the context of the macroscopic model, we should unambiguously clarify the symbols present in the macroscopic description. The force term prescribed by the authors [1, 2] for the **Herty-Illner Vlasov model** is:

$$B(\rho, v - \boldsymbol{u}^X) = \left\{ \begin{array}{ll} -g_1(\rho)(v - \boldsymbol{u}^X) & \text{if } v > \boldsymbol{u}^X \\ -g_2(\rho)(v - \boldsymbol{u}^X) & \text{if } v < \boldsymbol{u}^X \end{array} \right\} \tag{1.31}$$

Certainly other choices of the force term are possible (a discussion of the possibilities is omitted here). For the prescription above (1.31) the corresponding force term for the **Herty-Illner macroscopic model** is:

$$B(\rho, u - u^X) = \left\{ \begin{array}{ll} -g_1(\rho)(u - u^X) & \text{if } u > u^X \\ -g_2(\rho)(u - u^X) & \text{if } u < u^X \end{array} \right\} \tag{1.32}$$

where we note the change of dependence from v to the macroscopic quantity $u(x,t)$. Furthermore, for the macroscopic model the **macroscopic non-local average velocity** is the following quantity:

$$u^X(x,t) = u(x + H + Tu(x,t), t - \tau) \tag{1.33}$$

where, relative to (1.17), the change of dependence from v to the macroscopic quantity $u(x,t)$ is noted. Particularly noteworthy is the unusual non-local dependency of u^X in terms of u (involving a composition of u with a function of itself). This unusual dependency is really the cause of the mathematical difficulties soon to be encountered.

1.2.4 On The Choice of Force Term

Consideration of the model dynamics resulting from the activity of the force term motivate the development of the specifics thereof. In order to do so we first examine a simple force term:

$$B(\rho, u - u^X) = -g(\rho)(u - u^X) \tag{1.34}$$

given in [1] as a (rudimentary) precursor motivating the development of (1.32). As we shall see shortly (1.34) is in fact too simple (we note that, like (1.32), (1.34) is defined in terms of a proportionality to the relative velocity $(u-u^X)$ but, unlike (1.32) where different density dependent factors $g_1(\rho)$ and $g_2(\rho)$ are applied to differentiate between braking and acceleration cases, (1.34) is given in terms of just one density dependent factor $g(\rho)$).

For zero-order Taylor expansion with respect to u, taking (1.34) for the force term B in the macroscopic equations (1.20) yields the Burgers equation (i.e., for this choice of force term, the macroscopic model corresponds to the classic system for pressureless gas dynamics in one dimension). Furthermore, performing the Taylor expansion to linear order instead, the macroscopic equations (1.20) yield a model corresponding to that of Aw-Rascle [4] and Zhang [5]. The authors point out [1] that $g(\rho)$ is typically taken to be monotone increasing in the literature, e.g.:

$$g(\rho) = c\ \rho^{\gamma} (\gamma > 0). \tag{1.35}$$

The interpretation of the factor (1.35) is that, the higher the density, the higher the force a driver will apply (regardless of whether the force is a braking force or an acceleration force).

Certainly it is not realistic for drivers to accelerate harder in denser traffic, so this case makes apparent the deficiency in the lack of distinct treatment between braking and acceleration scenarios. This is the motivation for the proposition of separate treatment to the braking and acceleration scenarios, as in (1.32). The attention

to the Herty-Illner models with the force term prescribed as (1.32) warrants the establishment of some qualitative justification for a reasonable specification for (1.32), as follows.

1.2.5 On The Choice Of Braking And Acceleration Forces

Assuming that behaviour should be differentiated according to braking and acceleration scenarios, the authors justify a more specific choice for B which is simple and suffices to produce the desired behaviour. We should note that, in the following developments, the constant ρ_{max} is usually taken to be approximately $\frac{1}{L}$, where L is the vehicular length.

On The Choice Of Braking Force

Drivers will brake if drivers ahead are slower, in which case the force term in the braking scenario may be denoted $B = B(\rho, w)$, where

$$w := u - u^X > 0.$$

We should not expect braking to occur when the cars ahead travel at the same speed:

$$B(\rho, 0) = 0 \ \forall \ \rho \in [0, \rho_{max}].$$

We note that this simple assumption does not handle the possibility that the cars ahead might be travelling at the same speed, but are too close together.

Braking should also be unnecessary when a density gap is ahead:

$$B(0, w) = 0 \ \forall \ w \geq 0.$$

Likewise, this simple assumption neglects the possibility that, despite a density gap ahead, a driver might be travelling at an uncomfortably high speed (which would necessitate braking).

In addition, extending the same reasoning in the last two assumptions to the case of a density gap and zero relative velocity, we make the following prescriptions:

$$B(0,0) = B_\rho(0,0) = B_{\rho\rho}(0,0) = B_w(0,0) = B_{ww}(0,0) = 0.$$

That is, this represents the assumption that, without any compulsion to brake (or accelerate) due to relative velocity with respect to cars ahead, the driver applies no force. Furthermore, it is reasonable to assume that small changes to one coordinate (in isolation of the other coordinate) of the function $B(\cdot,\cdot)$ should not result in the application of any force, so it is reasonable to consider the corresponding partial derivatives to be equal to zero (1.2.5).

Assuming sufficient regularity in order that B may be expanded in a Taylor series, and truncated to second order, we have, approximately:

$$B(\rho,w) = B(0,0)+\rho B_\rho(0,0)+wB_w(0,0)+\frac{1}{2}\big[\rho^2 B_{\rho\rho}(0,0)+2\rho w B_{\rho w}(0,0)+w^2 B_{ww}(0,0)\big].$$

Since all terms except the cross-term are zero,

$$B(\rho,w) = B_{\rho w}(0,0)\rho w.$$

Moreover, choosing $c_1 = -B_{\rho w}(0,0)$ yields the ansatz given in [1]:

$$B(\rho, v-u^X) = -g_1(\rho)(v-u^X),$$

with $g_1 = c_1\rho$.

On The Choice Of Acceleration Force

Similarly in the acceleration scenario we may write $A = A(\rho,w)$ where $w<0$ and the assumptions corresponding to those made for the braking force may be tabulated:

$$\begin{aligned} A(\rho_{max},w) &= 0 \\ A(\rho,0) = 0 \Longrightarrow A(\rho_{max},0) &= 0. \end{aligned}$$

That is, the last discussion pertaining to braking revolved around the lack of necessity of braking in the situation for drivers experiencing negligible relative velocities and/or densities. Then the corresponding discussion in the acceleration situation refers to the lack of necessity of acceleration for drivers experiencing negligible relative velocities and/or high ("maximal") densities (i.e., in this context the implicit meaning of the "maximal" density coefficient $\rho_{\max}$ must be that: $\rho_{\max}$ represents some density threshold above which drivers would find it uncomfortable to accelerate further).

Analogously, making the generalization (as before) to the partial derivatives:

$$A_\rho(\rho_{max}, 0) = A_{\rho\rho}(\rho_{max}, 0) = A_w(\rho_{max}, 0) = A_{ww}(\rho_{max}, 0) = 0.$$

Expanding around $(\rho_{max}, 0)$, the formal Taylor expansion yields, to second order:

$$A(\rho, w) = A(\rho_{max}, 0) + (\rho - \rho_{max}) f_x(\rho_{max}, 0) + wA_w(\rho_{max}, 0)$$
$$+\frac{1}{2!}\Big[(\rho - \rho_{max})^2 A_{\rho\rho}(\rho_{max}, 0) + 2(\rho - \rho_{max}) wA_{\rho w}(\rho_{max}, 0) + w^2 A_{ww}(\rho_{max}, 0)\Big].$$

Then, as all terms but the cross term are zero,

$$A(\rho, w) = (\rho - \rho_{max}) wA_{\rho w}(\rho_{max}, 0).$$

Fixing $c_2 = A_{\rho w}(\rho_{max}, 0)$ yields a force for the acceleration case:

$$A(\rho, w) = c_2(\rho_{max} - \rho)w$$

where $w < 0$ and $g_2(\rho) = c_2(\rho - \rho_{max})$, matching the corresponding ansatz of [1]:

$$B(\rho, v - u^X) = -g_2(\rho)(v - u^X).$$

In conclusion, some rudimentary assumptions were presented on the properties of braking and acceleration forces necessitating that, in the second-order sense, the braking and acceleration forces should match the ansatz (1.32) given in [1] with:

$$\begin{aligned} g_1(\rho) &= c_1\rho \\ g_2(\rho) &= c_2(\rho - \rho_{max}). \end{aligned} \tag{1.36}$$

Discussion

In regard to the force terms developed so far Illner raises several concerns [2] as follows.

- Driver behaviours neglected so far in the modelling include and are not limited to: traffic rules such as speed limits, spontaneous acceleration in low density, spontaneous braking in high density, and noisy driving.

- The assumption $A(\rho, 0) = 0$ for small ρ ignores the possibility that acceleration

might occur in low density even though the lead car is not moving at a faster speed. That is, cars might move to fill gaps if the lead car is slow.

To motivate the further model developments and refinements which are presented in the final chapter, it is also important to mention the maximum principle associated with the Herty-Illner macroscopic model in the context of the force terms developed thus far.

1.2.6 Maximum Principles

We document the maximum principle as in [2] which reads: "there will be no deceleration below the lowest speed driven anywhere on the road at time zero, and no acceleration beyond the fastest such speed".

Assuming the Herty-Illner macroscopic model (1.20) in the context of the force term of type (1.32) where in particular $g_1(\rho)$ and $g_2(\rho)$ are given by (1.36), we have the system:

$$\begin{aligned} &\rho_t + (\rho u)_x = 0 \\ &u_t + uu_x + c_1\rho(u - u^X) = 0 \qquad\qquad (u - u^X \geq 0) \\ &u_t + uu_x + c_2(\rho_{max} - \rho)(u - u^X) = 0. \qquad\qquad (u - u^X < 0) \end{aligned} \tag{1.37}$$

Proposition: Supposing for all x and for all $s \in [0, \tau]$ we have $0 \leq a \leq u(x, s) \leq b$, then a smooth solution of (1.37) satisfies $0 \leq a \leq u(x, t) \leq b$ for all x and $t \geq 0$.

Proof: The switch between the braking and acceleration momentum-transfer equations in (1.37) occurs at isolated points. At such an isolated point where the model switch occurs there is a local maximum (minimum) in u. At such points $(u - u^X)$ vanishes. For the points leading up to such a maximum (minimum) where the acceleration (braking) version of the momentum-transfer equation applies, since $(u - u^X)$ is vanishing, none of the points experiencing the acceleration (braking) may accelerate (brake) to a speed above (below) the local maximum (minimum) speed. □

This principle rules out self-excitatory dynamics indicating the need of further refinements. Refinements to the above model [1] given in [2] shall not be given separate presentation. Instead, the most current developments of the Herty-Illner model [3] will be presented: this extends further the refinements made in [2]. These

refinements serve to partially address the concerns above, and in particular, address the need for driver behaviour to properly reflect density conditions.

Having placed the Herty-Illner macroscopic model in the second-order macroscopic modelling context (in particular, by developing the relationship with the established model of Aw-Rascle-Zhang for which formalization will be immediately forthcoming (1.3.2)), having showed the construction of the Herty-Illner macroscopic model from a kinetic perspective, and having presented some reasonably justifiable modelling choices, the preparations have been made for an investigation of the model dynamics, which will proceed forthwith. For the dynamics the subject of inquiry will be travelling wave solutions for the macroscopic model, representing moving traffic jams (moving "un-jam" waves) in the braking (acceleration) case. The remainder of this chapter considers approximate travelling wave solutions in relation to the exact travelling wave solutions, placing more emphasis on the approximate versions. The topic of exact travelling wave solutions is an open problem given greater attention in the second chapter.

1.3 Model Simplification By Series Approximation

The discussion of approximate travelling wave solutions begins with applying the Taylor series approach to the non-locality in the space variable. This provides some foothold to understanding the dynamics while (temporarily) avoiding the thornier problems inherent in the fully non-local system.

1.3.1 Non-locality Removal

As in [1] for the case $\tau = 0$ we reproduce the Taylor expansion of (1.37), i.e., the non-local Herty-Illner model (1.20) in the context of the usual force term:

$$B(\rho, u - u^X) = \begin{cases} -g_1(\rho)(u - u^X) & \text{if} \quad u - u^X > 0 \\ -g_2(\rho)(u - u^X) & \text{if} \quad u - u^X < 0. \end{cases} \tag{1.38}$$

with

$$\begin{aligned} g_1(\rho) &= c_1\rho \\ g_2(\rho) &= c_2(\rho_{max} - \rho). \end{aligned} \tag{1.39}$$

This Taylor expansion followed by truncation to second order results in a system (1.43) of partial differential equations of Hamilton-Jacobi type with diffusive correction [1].

The Taylor expansion proceeds case by case: $u > u^X$, $u < u^X$. In order to reach a simpler version of the force term involving u (but not the composition of u with itself), we approximate $w := u - u^X$ near $w = 0$. Certainly (1.38) has one-sided first and second order derivatives; here it is assumed that the one-sided first and second derivatives exist in general. For $w := u > u^X$ (braking) and $w := u < u^X$ (accelerating), respectively:

$$B(\rho, u - u^X) = B(\rho, 0^+) + B_u(\rho, 0^+)(u - u^X) + \frac{1}{2}B_{uu}(\rho, 0^+)(u - u^X)^2 + \dots \quad (1.40)$$

$$B(\rho, u - u^X) = B(\rho, 0^-) + B_u(\rho, 0^-)(u - u^X) + \frac{1}{2}B_{uu}(\rho, 0^-)(u - u^X)^2 + \dots . \quad (1.41)$$

If $B(\rho, w)$ is (1.38), for $u > u^X$, the first order truncation is exact: $B(\rho, u - u^X) = -g_1(\rho)(u - u^X)$ and $B(\rho, u - u^X) = -g_2(\rho)(u - u^X)$ for $u < u^X$.

Expanding $u - u^X$:

$$(u - u^X) = -u_x(H + Tu) - \frac{1}{2}u_{xx}(H + Tu)^2 + \dots \quad (1.42)$$

and assuming sufficient regularity, $u(x,t)$, $u^X(x,t)$, $u_x(x,t)$, and $u_{xx}(x,t)$ are evaluated at (x,t). For (1.38), removal of the non-locality via truncation cf. (1.42) suggests to replace (to first order accuracy) $u - u^X > 0$ by $u_x < 0$ (and $u - u^X < 0$ by $u_x > 0$). Making this assumption and, where $i = 1$ for $u_x < 0$ and $i = 2$ for $u_x > 0$, we can summarize an approximate model by applying (1.40), (1.41), and (1.42) to (1.20) with (1.38) as the following system of equations (which is of Hamilton-Jacobi type with diffusive correction):

$$\begin{aligned} \rho_t + (\rho u)_x &= 0 \\ u_t + uu_x - g_i(\rho)[u_x(H + Tu) + \frac{1}{2}u_{xx}(H + Tu)^2] &= 0. \end{aligned} \quad (1.43)$$

Before proceeding to the comparison of the full system with its approximation (1.43) via the travelling-wave-solution concept (1.4) we state an immediate consequence of the above.

1.3.2 Reproduction of The Aw-Rascle-Zhang Model

For the macroscopic model with $\tau = 0$, taking $B(\rho, u - u^X) = -g_1(\rho)(u - u^X)$ (the force term representative of the braking case only) and the Taylor expansion:

$$(u - u^X) = -u_x(H + Tu) + \dots$$

leads us to arrive at the following simplified momentum equation:

$$u_t + uu_x - g_1(\rho)(H + Tu)u_x = 0. \tag{1.44}$$

Setting $\frac{\partial}{\partial\rho}p = p_\rho(\rho, u) = \frac{g_1(\rho)}{\rho}(H + Tu)$, an analog of the momentum equation associated with the model of Aw, Rascle, and Zhang: $u_t + uu_x + \rho\partial_\rho p(\rho)u_x = 0$ is recovered, with the exception that, for the "pressure law"[3] we have $p = p(\rho, u)$ instead of $p = p(\rho)$.

Thus the momentum expression analogous to that of the Aw-Rascle-Zhang model recovered is:

$$u_t + uu_x + \rho\partial_\rho p(\rho, u)u_x = 0$$

In summary, the usual mass law combined with the above momentum transfer law (1.44) recovers an Aw-Rascle-Zhang type model from the Herty-Illner macroscopic model (in the braking case and for $\tau = 0$) by Taylor expansion of the latter (with truncation to linear order).

1.4 (Un-)Jam Equations & Approx. Analogs Thereof

In addition to the ordinary differential equations (1.43) just derived, the full non-local model (1.37) is compared with two further simplified versions:

- the ordinary differential equations (1.50,1.52) associated with the (exact) travelling-wave solutions of the full model (1.37), and,
- (1.53,1.54) representing localized versions of the ordinary differential equations (1.50,1.52) in a more tractable form.

[3]Please see the footnotes below (1.6).

This is accomplished by taking fully non-local model before truncation (1.37), i.e., the macrocsopic model (1.20) in the context of the specific force term (1.38), stating the travelling wave solution hypothesis (1.45) which, in application to the full partial differential equation model (1.37) yields the ordinary differential equations (1.50) and (1.52): one for each of the cases in (1.37).

1.4.1 Travelling Wave Hypothesis

Given the continuity equation $\rho_t + (\rho u)_x = 0$ the travelling wave assumption (where $V > 0$ is assumed to limit the discussion so that it is only representative of backwards-moving waves) is given by the following system of equations:

$$\begin{aligned} \rho(x,t) &= \rho(x+Vt) \\ u(x,t) &= u(x+Vt). \end{aligned} \tag{1.45}$$

Here the quantity $s = x+Vt$ is referred to as the wave coordinate. For the continuity equation this yields the relationship

$$\frac{d}{ds}(\rho(u+V)) = 0. \tag{1.46}$$

1.4.2 Continuity Equation For Travelling Waves

Integrating (1.46) and expressing the constant of integration as a product of V (for convenience),

$$\begin{aligned} \rho(s)(u(s)+V) &= c_0 V \qquad\qquad (u(s)+V>0) \\ \implies \rho(s) &= \frac{c_0 V}{u(s)+V}. \end{aligned} \tag{1.47}$$

On the basis of the understanding offered, we note a relevant assumption [1] and consequence:

$$(\rho = \rho_{max} \to u = 0) \to c_0 = \rho_{max}. \tag{1.48}$$

That is, the assumption that traffic has stopped moving at the so-called "maximal-density" $\rho_{\max}$, leads to the conclusion that the constant c_0 be equal to $\rho_{\max}$.

In the proceedings we neglect this kind of assumption (to avoid losing some modicum of generality).

1.4.3 The Jam and Unjam Equations

As indicated, Herty and Illner combine the travelling wave hypothesis with the model equations for the braking and acceleration cases, resulting in the two equations called the **jam** and **unjam** equations, respectively. In light of ongoing refinements to the modelling, we note the possibility of investigating the travelling wave hypothesis in the context of different force term cases (a suggestion not pursued here).

At this stage the introduction of the jam and unjam equations is appropriate; since their non-trivial solution represents a fascinating problem of practical and theoretical interest, they will be given our undivided attention in the second chapter.

1.4.4 Jam Equation

The model equations for (1.20) with (1.38) and (1.39) are, for braking ($u - u^X > 0$):

$$\begin{aligned} \rho_t + (\rho u)_x &= 0 \\ u_t + u_x u + c_1 \rho (u - u^X) &= 0. \end{aligned} \tag{1.49}$$

The wave ansatz is $\rho(x,t) = \rho(x+Vt)$, $u(x,t) = u(s) = u(x+Vt)$ with wave coordinate $s = x + Vt$, so we have the relations $\frac{\partial s}{\partial t} = V$, $\frac{\partial t}{\partial s} = \frac{1}{V}$, and $\frac{\partial s}{\partial x} = 1$.

$$\begin{aligned} u^X(x,t) &= u(x + H + Tu(x,t), t - \tau) \\ &= u(x + H + Tu(x+Vt) + V(t-\tau)) \\ &= u(s + H + Tu(s) - \tau V)). \end{aligned}$$

Using also the above expression for u^X, recalling (1.47), and observing that $\frac{\partial}{\partial x} u = \frac{\partial}{\partial s} u$, $\frac{\partial}{\partial t} u = V \frac{\partial}{\partial s} u$, we rewrite (1.49) as:

$$\begin{aligned} \rho(s) &= \frac{c_0 V}{u(s) + V} \\ 0 &= V \frac{d}{ds} u + u \frac{d}{ds} u + c_1 \rho (u - u^X) \end{aligned}$$

to obtain the **jam equation:**

$$\big(V + u(s)\big)^2 u'(s) = -c_1 c_0 V[u(s) - u(s + (H - \tau V) + Tu(s))]. \tag{1.50}$$

1.4.5 Unjam Equation

In (1.49) for acceleration ($u - u^X < 0$) the model equations for (1.20) with (1.38) and (1.39), the momentum law is instead:

$$u_t + u_x u + c_2(\rho_{max} - \rho)(u - u^X) = 0. \tag{1.51}$$

We derive for (1.51) in analogy with (1.50) the **unjam equation:**

$$\big(V + u(s)\big)^2 u'(s) = -c_2(\rho_{max}(u(s) + V) - c_0 V)[u(s) - u(s + (H - \tau V) + Tu(s))]. \tag{1.52}$$

For generality we keep (1.52) noting that (1.48) allows further simplification:

$$\big(V + u(s)\big)^2 u'(s) = -c_2 \rho_{max} u(s)[u(s) - u(s + (H - \tau V) + Tu(s))].$$

1.4.6 Truncation of Jam Equations: Localized Waves

Having introduced the jam and unjam equation, respectively:

$$\big(V + u(s)\big)^2 u'(s) = -c_1 c_0 V[u(s) - u(s + (H - \tau V) + Tu(s))]$$
$$\big(V + u(s)\big)^2 u'(s) = -c_2(\rho_{max}(u(s) + V) - c_0 V)[u(s) - u(s + (H - \tau V) + Tu(s))]$$

we develop a test to establish a sense of consistency with their approximate analogs (cf. the truncated model (1.43)) as we will elaborate. In particular, we treat the above with a Taylor series expansion and second-order truncation:

$$u(s + (H - \tau V) + Tu(s)) \simeq u(s) + u'(s)(H - \tau V + Tu(s)) + \frac{1}{2}u''(s)(H - \tau V + Tu(s))^2$$
$$u(s) - u(s + (H - \tau V) + Tu(s)) \simeq -\bigg[u'(s)(H - \tau V + Tu(s)) + \frac{1}{2}u''(s)(H - \tau V + Tu(s))^2\bigg],$$

becoming:

$$\big(V+u\big)^2u' - c_1c_0V\bigg[u'(H-\tau V+Tu)+\frac{1}{2}u''(s)(H-\tau V+Tu)^2\bigg]=0$$
$$\big(V+u\big)^2u' - c_2(\rho_{max}(u+V)-c_0V)\bigg[u'(H-\tau V+Tu)+\frac{1}{2}u''(s)(H-\tau V+Tu)^2\bigg]=0.$$

Rearranging into the normal form for second order ordinary differential equations:

$$u''=2u'\frac{\big(V+u\big)^2-c_1c_0V(H-\tau V+Tu)}{c_1c_0V(H-\tau V+Tu)^2} \tag{1.53}$$
$$u''=2u'\frac{\big(V+u\big)^2-c_2(\rho_{max}(u+V)-c_0V)(H-\tau V+Tu)}{c_2(\rho_{max}(u+V)-c_0V)(H-\tau V+Tu)^2}. \tag{1.54}$$

Recapitulating, the above represents 1) applying the travelling wave assumption followed by 2) a Taylor expansion (and truncation) to the non-locality.

The sense of consistency we establish[4] is that (in the case $\tau=0$ only) the ordinary differential equations above match those derived from applying to the full model, the same two steps in reverse, i.e., 1) applying a Taylor expansion (and truncation) of the non-locality to obtain the truncated model (1.43) followed by 2) application of the travelling wave assumption. To complete this, the item outstanding is the insertion of the travelling wave hypothesis (cf. the resulting continuity equation) as follows. □

Waves for the Hamilton-Jacobi form

From the truncated model (1.43) we reproduce the second order ordinary differential equations used in [1] to study the phase-plane dynamics of (travelling) braking waves. In the case that $\tau=0$, we will see that the second order ordinary differential equations produced here match those seen before (1.53,1.54). The reproduction is performed in both cases by manipulating (1.43) to solve for u_{xx}:

$$\frac{g_i(\rho)}{2}u_{xx}(H+Tu)^2=u_t+uu_x-g_i(\rho)u_x(H+Tu)$$
$$u_{xx}=2\frac{u_t+uu_x-g_i(\rho)u_x(H+Tu)}{g_i(\rho)(H+Tu)^2}$$

[4]Doing this presupposes that, to the commutativity question for the two operations, there is not an affirmative answer which is immediately obvious. For the simplification procedure, a negative answer would suggest the need for more rigorous justification for the order of operations used, and a comparison of the results. Indeed, for the case $\tau\neq 0$, such a comparison has not been considered.

and with (for convenience only) the shorthand $\Delta := (H + Tu(s))$:

$$u_{xx} = 2\frac{u_t + uu_x - g_i(\rho)u_x\Delta}{g_i(\rho)\Delta^2}$$

Substituting $\rho(s) = \frac{c_0 V}{u(s)+V}$ the continuity equation (1.47) for the travelling wave ansatz (V is the wave speed) and $ds = dx$ and $dt = \frac{ds}{V}$ pertaining to the wave coordinate s cf. (1.45), using the shorthand $A := u(s) + V$:

$$\frac{d^2}{ds^2}u(s) = 2\frac{V \cdot \frac{d}{ds}u(s) + u(s) \cdot \frac{d}{ds}u(s) - g_i(\frac{c_0 V}{u(s)+V})\Delta\frac{d}{ds}u(s)}{g_i(\frac{c_0 V}{u(s)+V}) \cdot \Delta^2}$$

$$u''(s) = 2u'(s)\frac{A - g_i(\frac{c_0 V}{A}) \cdot \Delta}{g_i(\frac{c_0 V}{A}) \cdot \Delta^2}$$

$$u''(s) = 2u'(s)\frac{A^2 - A \cdot g_i(\frac{c_0 V}{A}) \cdot \Delta}{A \cdot g_i(\frac{c_0 V}{A}) \cdot \Delta^2}$$

where again, $g_1(\rho) = c_1\rho$ and $g_2(\rho) = c_2(\rho_{max} - \rho)$. Thus,

$$u''(s) = 2u'(s)\frac{(u(s)+V)^2 - c_2(\rho_{max}(u(s)+V) - c_0 V)(H + Tu(s))}{c_2(\rho_{max}(u(s)+V) - c_0 V)(H + Tu(s))^2}. \tag{1.55}$$

$$u''(s) = 2u'(s)\frac{(u(s)+V)^2 - c_1 c_0 V(H + Tu(s))}{c_1 c_0 V(H + Tu(s))^2} \tag{1.56}$$

for the acceleration (1.55) and braking (1.56) cases, respectively. Evidently for $\tau = 0$ in (1.53,1.54) the equations (1.55,1.56) match (1.53,1.54).

1.5 Localized Travelling Waves Exist For The Model

Here we reproduce the travelling wave (1.47) solution existence theorem that was given in [1] for the Hamilton-Jacobi form of the traffic model (1.43), with the exception that the principle will be formulated using the ordinary differential equations (1.53,1.54) rather than (1.43) cf. [1]. Again (for the case $\tau = 0$ only) the same ordinary differential equations (1.55,1.56) were recovered (1.53, 1.54) from the partial differential equation model with application of the simplifying steps in the reverse order: that is, application of the travelling-wave assumption before using a Taylor-series truncation.

The introduction of the time delay τ, neglect of the assumption $c_0 = \rho_{\max}$ (1.48), and the emphasis on the acceleration scenario, all represent slight extensions to the principle [1] that (localized) travelling wave solutions exist for the macroscopic traffic model (1.20).

Phase Plane Analysis

If $\Delta := ((H - \tau V) + Tu)$ we adopt for (1.53,1.54) the F_a and F_b notation:

$$F_a(u) := 2\frac{(u+V)^2 - c_2(\rho_{max}(u+V) - c_0 V)\Delta}{c_2(\rho_{max}(u+V) - c_0 V)\Delta^2} \tag{1.57}$$

$$F_b(u) := 2\frac{(u+V)^2 - c_1 c_0 V \Delta}{c_1 c_0 V \Delta^2} \tag{1.58}$$

For structure we analyze in $u(s)$ and $z(s) := u'(s)$ (the phase plane):

$$\frac{dz}{du} = F_a(u) \ (z > 0). \tag{1.59}$$

$$\frac{dz}{du} = F_b(u) \ (z < 0) \tag{1.60}$$

Travelling Wave Solutions (Phase Plane)

An acceleration {braking} travelling wave solution (cf. [1]) is a parameterized curve $(u(s), z(s))$ in s with the following properties:

$$\begin{array}{rrrr}
u(-\infty) & = u_0 & \{u(\infty) & = u_0\} \\
z(-\infty) & = 0 & \{z(\infty) & = 0\} \\
\forall s : u'(s) & = z(s) > 0 & \{\forall s : u'(s) & = z(s) < 0\} \\
\lim\limits_{s\to\infty} u(s) & = u_\infty < \infty & \{\lim\limits_{s\to-\infty} u(s) & = u_{-\infty} < \infty\} \\
\lim\limits_{s\to\infty} z(s) & = 0 & \{\lim\limits_{s\to-\infty} z(s) & = 0\}.
\end{array} \tag{1.61}$$

An acceleration {braking} travelling wave solution is said to connect the states u_0 and u_∞ $\{u_0$ and $u_{-\infty}\}$.

Proposition: Existence Of (Localized) Travelling Wave Solutions

(A) For $c_2\rho_{\max}T > 1$, there exists an α such that[5], for initial data u_0 (1.62) with $u_0 < \alpha$, and wave speeds V satisfying:

$$\frac{c_2(\rho_{\max} - c_0)H}{1 + c_2(\rho_{\max} - c_0)\tau} < V < \frac{H}{\tau}$$

there is a (localized) acceleration travelling wave solution for the system (1.20) beginning with

$$u_0 = \inf_s u(s). \tag{1.62}$$

(B) For all u_0 (1.62) there is a β such that[6], for initial data u_0 (1.62) with $u_0 < \beta$, and wave speeds V satisfying:

$$0 < V < \frac{c_0c_1H}{(1 + c_0c_1\tau)} < \frac{H}{\tau}$$

there is a (localized) braking (deceleration) travelling wave solution for the system (1.20) ending with u_0.

It is assumed that the constants $H, T, \tau, c_0, c_1, c_2, V$ are all positive, and also that (1.63) and (1.64).

$$0 < H - \tau V \qquad \text{(Causality)} \tag{1.63}$$

$$c_0 < \rho_{\max} \qquad \text{(Density of Standing Traffic)} \tag{1.64}$$

Proof

Noting (1.63) and (1.64) we see that both $F_b(u)$ (the right hand (1.58) of (1.60)) and $F_a(u)$ (the right hand (1.57) of (1.59)) have positive and monotonically increasing

[5]The parameter α is given at the end of the proof (1.68)

[6]The parameter β is also given at the end of the proof (1.69). The parameters α and β represent bounds on the speed profile (for the acceleration and braking cases, respectively) in terms of the wave speed V as well as the model parameters: $\tau, c_0, c_1, c_2, H, V, T, \rho_{\max}$.

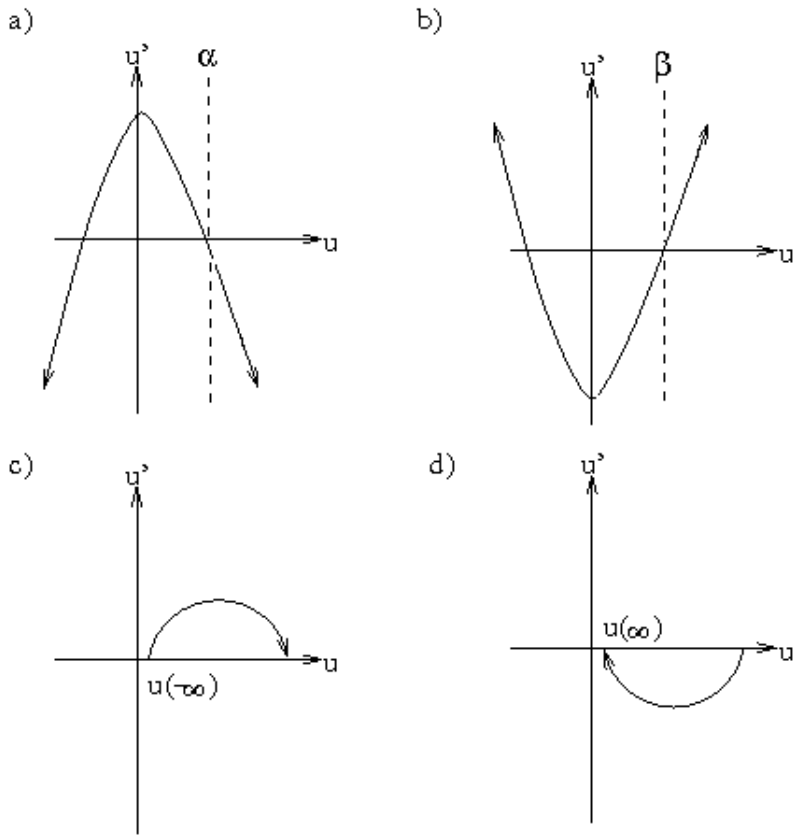

Figure 1.1: Quantities Pertinent To The Study Of (Localized) Travelling Wave Solutions

denominators. The numerators $N_b(u)$ and $N_a(u)$ for F_b and F_a are:

$$\begin{aligned}
N_b(u) &= (u+V)^2 - c_1c_0V((H-\tau V)+Tu) \\
&= u^2 + u\cdot V(2-c_1c_0T) + V(V-c_1c_0(H-\tau V)) \\
N_a(u) &= (u+V)^2 - c_2(\rho_{max}(u+V)-c_0V)((H-\tau V)+Tu) \\
&= u^2\cdot(1-c_2\rho_{max}T) + u\cdot(V(2-c_2T(\rho_{max}-c_0)) - c_2\rho_{max}\delta) + V(V-c_2(\rho_{max}-c_0)\delta)
\end{aligned}$$

where the shorthand $\delta := H - \tau V$ was used. $N_b(u)$ is a parabola opening up (see **b)** in Fig. (1.1)) with $N_b(0) < 0$ provided that $V - c_1c_0(H-\tau V) < 0$ or, equivalently

$$V < \frac{c_1c_0H}{(1+c_1c_0\tau)}.$$

Since $0 < V$ we re-state the required bound on V as:

$$0 < V < \frac{c_1 c_0 H}{(1 + c_1 c_0 \tau)}. \tag{1.65}$$

$N_a(u)$ is a parabola opening down provided $c_2 \rho_{max} T > 1$. If in addition, using the shorthand $\gamma := c_2(\rho_{\max} - c_0)$ (we already noted $\gamma > 0$) then $V(V - c_2(\rho_{max} - c_0)\delta) > 0$ or, equivalently $V > \frac{\gamma H}{1+\gamma\tau}$, i.e.,

$$V > \frac{c_2(\rho_{\max} - c_0)H}{1 + c_2(\rho_{\max} - c_0)\tau}. \tag{1.66}$$

For (1.66) $N_a(u)$ is a parabola opening down with $N_a(0) > 0$ ((see **a)** in Fig. (1.1)). This and (1.66) {(1.65)} for the acceleration {braking} case allow the following conclusions. For the acceleration case, $F_a(0) > 0$ and there exists $\alpha > 0$ such that {for the braking case, $F_b(0) < 0$ and there exists $\beta > 0$ such that}:

- $F_a(\alpha) = 0$ $\{F_b(\beta) = 0\}$
- $0 < u < \alpha \rightarrow F_a(u) > 0$ $\{0 < u < \beta \rightarrow F_b(u) < 0\}$, and
- $u > \alpha \rightarrow F_a(u) < 0$ $\{u > \beta \rightarrow F_b(u) > 0\}$.

Here we observe that α, β represent the position on the $u-$axis where $N_a(u)$, $N_b(u)$ (and hence $F_a(u), F_b(u)$) change sign. Then for every $u_0 < \alpha$ $\{u_0 < \beta\}$ there is some finite $u_\infty > \alpha$ $\{u_{-\infty} > 0\}$ such that:

- $F_a(u_0) > 0$ $\{F_b(u_0) < 0\}$,
- $F_a(u_\infty) < 0$ $\{F_b(u_{-\infty}) > 0\}$, and
- $\int_{u_0}^{u_\infty} F_a(u)du = 0$ $\{\int_{u_0}^{u_{-\infty}} F_b(u)du = 0\}$.

Then the phase-plane coordinate $z(u)$ for the acceleration {braking} case:

$$z(u) = \int_{u_0}^{u} F_a(\xi)d\xi \quad \left\{ z(u) = \int_{u_0}^{u} F_b(\xi)d\xi \right\} \tag{1.67}$$

represents an acceleration {braking} travelling-wave solution (1.61) connecting u_0 and u_∞ {u_0 and $u_{-\infty}$} (see **c)** {**d)**} in Fig. (1.1)). □

Conclusion

The parameters α and β are, where $\xi_\alpha = V(c_0c_2T - 2)$, $\xi_\beta = V(c_0c_1T - 2)$, and $\gamma = c_2(\rho_{\max} - c_0)$:

$$\alpha = -\frac{\xi_\alpha + c_2\rho_{\max}(H + V(T-\tau))}{2(c_2\rho_{\max}T - 1)} - \sqrt{\left(\frac{\xi_\alpha + c_2\rho_{\max}(H + V(T-\tau)))}{2(c_2\rho_{\max}T - 1)}\right)^2 + \frac{V(V(1+\gamma\tau) - \gamma H)}{(c_2\rho_{\max}T - 1)}} \tag{1.68}$$

$$\beta = \frac{1}{2}\xi_\beta + \sqrt{\left(\frac{1}{2}\xi_\beta\right)^2 + V(c_1c_0H - V(1 + c_1c_0\tau))}. \tag{1.69}$$

In summary, we have the following inequalities for acceleration ($c_0 < \rho_{\max}$):

$$c_2\rho_{\max}T > 1; \qquad \frac{\gamma H}{1+\gamma\tau} = \frac{c_2(\rho_{\max} - c_0)H}{1 + c_2(\rho_{\max} - c_0)\tau} < V < \frac{H}{\tau} \tag{1.70}$$

and braking:

$$0 < V < \frac{c_0c_1H}{(1 + c_0c_1\tau)} < \frac{H}{\tau}. \tag{1.71}$$

Discussion

Foreshadowing the conclusions of the third and final chapter we note that, relative to the original version of this proof, [1] the addition of the reaction time parameter τ (which is expected and is observed in reality) really forces us to re-evaluate the validity range of the modelling. This is apparent from the revised inequalities (1.70),(1.71). Here we elaborate upon the meaning of the statement with the assistance of numerical integrations (1.2, 1.3, 1.4) representing approximate solutions to the ordinary differential equations (1.60),(1.59) in phase-space $(u, z = u')$. For the figures (1.2, 1.3, 1.4) u' appears on the vertical axis whereas u appears on the horizontal axis. Numerical integration curves corresponding to the braking case (1.60) are shown in red, whereas numerical integration curves corresponding to the acceleration case (1.59) are shown in green.

Points on the u axis represent equilibria ($z = u' = 0$). Of course the ordinary-differential-equation model guarantees the inescapability (in finite time) from equilibra (despite, in general, the obvious instability due to the switching between F_a and

F_b across the $z-$axis) and the exponential behaviour near equilibria (whether growing or decaying). Consequently the model, while lending a qualitatively reasonable description of travelling wave dynamics (for braking and acceleration scenarios), is not intended to provide justification or explanation for the origin of the waves.

Undoubtably waves are due to perturbations (triggers) in traffic conditions which remain un-accounted for in the modelling: such departures from the current state of affairs may be expected (e.g. fixed variations in the physical landscape: lane reductions or expansions, traffic control devices) or not (e.g., complicated features of the dynamical landscape of human decision-making that are likely outside our realm of understanding). A partial solution to this problem is the propensity to account for perturbations or other traffic features, by representing them in terms of the initial conditions (this solution does not apply, should the departure from "business as usual" involve a departure from the usual driver behaviour, which might need to addressed by using alternative force terms). The necessity of triggers is a reminder that the model should be taken with a grain of salt. The fact that the model does not account for the possibility of "escape" from the equilibria is another such reminder. Nevertheless the model represents a simple theoretical avenue for the derivation of parameters to assist in the development of plans for traffic control and/or state prediction, motivated by reasonable modelling considerations.[7]

The travelling waves are heteroclinic orbits (that is, phase-space trajectories connecting one equilibrium to another). The acceleration wave starts at a given equilibrium $(u_0 > 0, z = 0)$ ending at another $(u_\infty, z = 0)$ of higher $u-$value (cf. Fig. (1.1):(c)), whereas the braking wave starts at a given equilibrium $(u_0 > 0, z = 0)$ ending at another $(u_{-\infty}, z = 0)$ of lesser $u-$value (cf. Fig. (1.1):(d)).

Accordingly the parameters α and β represent the location on the $u-$axis where the functions F_a and F_b change sign (from positive to negative for F_a as in Fig. (1.1):(a) and, from negative to positive for F_b as in Fig. (1.1):(b)). Then, α and β represent the local extrema for the phase plane curves $z(u)$ (cf. Fig. (1.1):(c),(d)) given as the integration (1.67) of the F_a, F_b.

Naturally it was necessary to seed numerical integrations at points slightly above the $u-$axis in order that the procedure terminate finitely. Numerical integrations in phase space (1.2, 1.3, 1.4) are supplied using the following fixed parameter settings: $H = 10$, $\rho_{\max} = 1$, $T = 2$, $c_0 = 0.9$, $c_1 c_0 = 1.6$, $c_2 = 1$. The other parameters of the

[7]Future work should include studies pursuing the empirical validation of the effectiveness of the parameters, for limiting (and/or predicting) the emergence of jams and/or stop-and-go waves.

integrations which were varied are tabulated in Table (1.1). As indicated in Table (1.1), the integrations within (1.2, 1.3, 1.4) correspond to $\tau = 0, \frac{1}{4}, \frac{1}{2}$ respectively. Within each of (1.2, 1.3, 1.4) the three panels (from left to right) represent integrations carried out using the three wave speeds $V = 6, 8, 9.5$ respectively.

Within each of the nine panels (with the exception of the last) two integrations are shown (in green) for initial values slightly above the $u-$axis (corresponding to the acceleration scenario) and two integrations are shown (in red) for initial values slightly below the $u-$axis (corresponding to the braking scenario). The initial values for those integrations representative of acceleration are chosen such that they correspond roughly with the (approximate) final values for the associated integrations representative of braking (we discuss the motivation for doing so in the next paragraph).

Violation of the existence inequality (1.71) is the situation depicted in the last panel of Fig. (1.4) ($\tau = \frac{1}{2}, V = 9.5$) for which $V = 9.5$ and $\frac{c_0 c_1 H}{(1+c_0 c_1 \tau)} = 8.88$ (shown in bold in Table (1.1)). In this last panel we observe that the integrations shown are, as we should expect according to (1.71), unrepresentative of the desired travelling wave solutions. Indeed, instead of approaching the equilibria, the integrations turn away and cross the $z-$axis. In this case, due to the violation of the existence critera in the braking case, we did not plot any integrations for acceleration.

Moreover, pertaining to the existence criteria for the acceleration case, we note that $c_2 \rho_{\max} T = 2 > 1$ so that, along with the fact that $\frac{\gamma H}{1+\gamma\tau}$ was small in magnitude, the existence critera for the phase-plane acceleration waves were satisfied throughout.

For each integration shown in the braking case representative of an (approximate) travelling wave solution (that is, for all of the integrations in red, with the exception of those in the last panel) integrations for the acceleration case were initiated with values representative of a small $z-$perturbation away from the (approximate) end-point corresponding to the braking case integration. That is, the succession of (approximate) braking solution followed by and (approximate) acceleration solution represents the concatenation of braking wave followed by acceleration wave necessary for the (approximate) representation of idealized stop-and-go waves. The circumstances consistent with the emergence of persisent stop-and-go waves then correspond to parameterizations representative of the case where the terminal point of the acceleration wave is the same as the initial point of the braking wave (and vice-versa) i.e., the heteroclinic orbits connect in a loop (such a situation is approximately depicted in the right-hand panel of (1.2) for the inner-most pair of concatenated integrations. In

contrast, the left-most and centre panels of (1.2) show a situation approximately representative of the successive concatenation of braking and acceleration waves, where the oscillations fade away. The left-most panel of Fig. (1.3) shows mixed behaviour where the wave concatenations may decay in magnitude for some initial states, but grow in amplitude for other initial states. On the other hand, the integrations shown in the centre and right-most panels of Fig. (1.3) and the first two panels of Fig. (1.4) show such (approximate) wave connections where the amplitude of the successive waves is increasing.

As in [1] we observe that if $u_0 < \min\{\alpha, \beta\}$ then the braking waves and acceleration waves connect. If so then if, in addition, $\beta > \alpha$ then the situation is stable, in the sense that the range $\alpha < u < \beta$ for the speed variable u is stable within the class of travelling wave solutions with group speed V. Otherwise for $\beta < \alpha$ the situation is not stable in that sense. We observe from the formulae (1.69) for the parameters that: increasing τ results in decreasing β and increasing α. Thus the stability prediction in terms of τ conferred by the updated formulae for α, β is consistent with the observation from the numerics: that increasing τ results in increasingly large unstable parameter domains. The conclusion in [1] which presents the potential use of α, β by traffic systems to avoid stop-and-go waves associated with a given speed V, is augmented by the observations here that the reaction time parameter τ strongly affects the associated stability regimes. Again, the inclusion of the reaction time parameter τ (which is expected and is observed in reality) emphasizes the importance of paying close attention to the parameter ranges for which the model is valid.

While the approximate (localized) equation gives a starting point for analyzing the dynamics, the non-locality should be necessary for a realistic description of traffic, as drivers react to what they observe ahead. Since the errors relative to the non-local system are substantial as seen from travelling wave profiles [9] and since the consideration of the non-local system gives rise to new and challenging mathematical problems, the non-locality is an object worthy of our attention.

Fig.		(1.2)	(1.3)	(1.4)
Parameter	τ	0	$\frac{1}{4}$	$\frac{1}{2}$
	V	6 8 9.5	6 8 9.5	6 8 ***9.5***
	$\frac{H}{\tau}$	∞	40	20
	$\frac{c_0 c_1 H}{(1+c_0 c_1 \tau)}$	16	11.42	8.88
	$\frac{\gamma H}{1+\gamma\tau}$	0.10	0.09	0.09

Table 1.1: Parameters employed in the numerical integrations representative of approximate (Localized) Travelling Wave Solutions shown in Figures (1.2),(1.3), and (1.4)

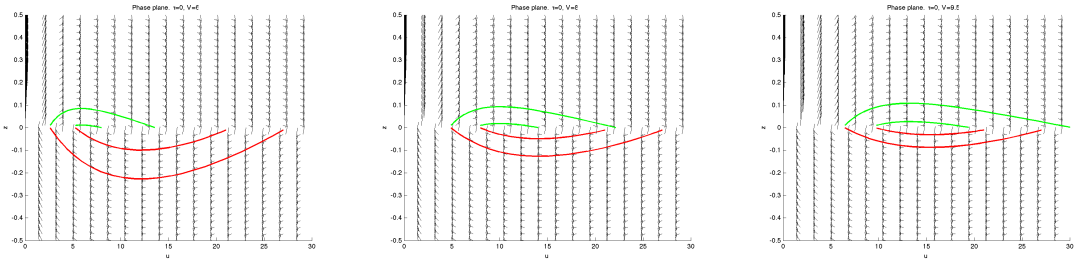

Figure 1.2: "Localized" Waves (green: accel., red:braking): $\tau = 0, V = 6, 8, 9.5$

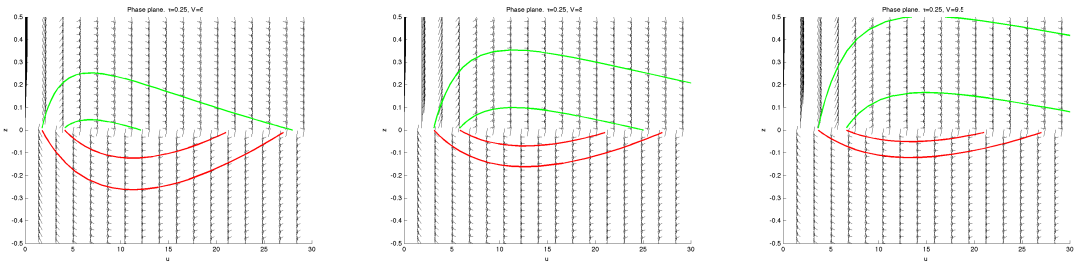

Figure 1.3: "Localized Waves" (green: accel., red:braking): $\tau = \frac{1}{4}, V = 6, 8, 9.5$

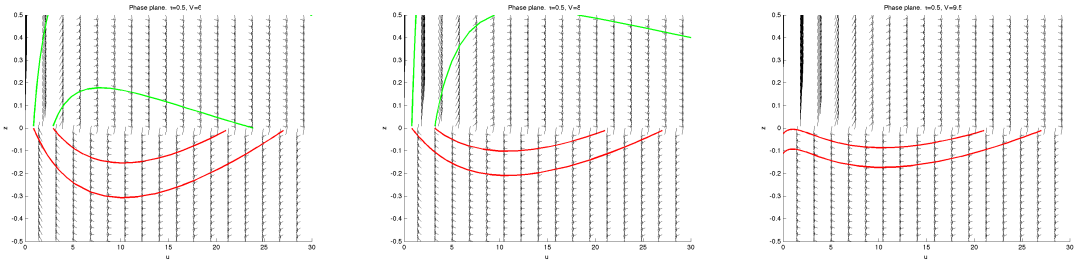

Figure 1.4: "Localized" Waves (green: accel.,red:braking): $\tau = \frac{1}{2}, V = 6, 8, 9.5$

Chapter 2

Functional Differential Equations

2.1 Introduction

Functional-equations are equations giving an implicit description of the unknown function(s), for example: the equation may determine the value assumed by the unknown function at a given point in terms of the values assumed by the unknown function at one or more other points. The **Cauchy functional-equation** [32]:

$$f(x+y) = f(x) + f(y)$$

is a prominent classical functional-equation.

The **jam equation** (1.50) and **unjam equation** (1.52):

$$\begin{aligned} \big(V+u(s)\big)^2 u'(s) + c_1 c_0 V(u(s) - u(s+H+Tu(s)-\tau V)) &= 0 \\ \big(V+u(s)\big)^2 u'(s) + c_2(\rho_{max}(u(s)+V) - c_0 V)(u(s) - u(s+H+Tu(s)-\tau V)) &= 0 \end{aligned} \tag{2.1}$$

are such equations, derived from the travelling wave assumption (1.45) applied to the Herty-Illner macroscopic traffic model equations in the braking case (1.49) and acceleration case (1.51), respectively. Since the equations feature composition of the unknown with quantites involving itself, the term **iterated** applies; such functional composition cf. $u(s+H+Tu(s)-\tau V)$ is an important distinction from the classical ordinary differential equations.

In the differential equations community, the term **state-dependent-arguments** is often used to refer to this kind of iteration. The more general term **delay-**

equations, that refers to equations whose arguments are subject to any kind of transformation, does include the situation where iteration is included. More frequently, the term **delay-equations** describes equations with arguments subject to transformations more elementary than iteration (e.g., linear transformations, or perhaps composition with known functions). Since the equations (2.1) generalize upon the simpler, better studied cases just mentioned, to distinguish (2.1) the descriptor **iterated-functional-differential-equations** is useful.

We mention Hale's monographs on **functional-delay-equations** [6, 33] noting that many other modern treatments of the topic are available as well as those generalized to other contexts e.g. that of partial-differential-equations [34]. Treatment of the more difficult subject of state-dependent arguments is less commonplace. State-dependence (i.e., the case where the unknown is transformed by some function of itself) is extremely delicate; in [8] a theory is presented for the latter - for example, the answer to the existence question is well known for simple iterative dependencies, e.g. the differential equation:

$$x'(s) = x(x(s)). \tag{2.2}$$

More exotic dependencies lead to greater challenge: the equations (2.1) are no exception. For (2.1) this is owing to the effective dependency (cf. the equivalent expressions (2.9,2.10)) of the form:

$$z'(s) = y[s, z(s)] \cdot [z(s + z(s)) - z(s)]. \tag{2.3}$$

For (2.3) the $y[s, z(s)]$ to be considered[1] is some functional of s and $z(s)$.

Perplexingly, in association with non-convergence of the series solution, the analytic series expansion methods [8] are not applicable to the two equations of interest. Thus the jam and un-jam equations resulting from the applied traffic problem considered here are also representative of a challenging (open) problem in the realm of pure mathematics. Before revisiting this problem and emphasizing some of the challenges involved we derive the associated forms (2.3) to facilitate the investigation of (2.1).

[1]The instances of (2.3) to be considered shall include the functional equations (2.9,2.10) that correspond to the un-jam and jam equations, respectively.

2.2 Simplifying the Traffic Functional-Equations

Here functional-differential-equations (2.1) revealed by applying a travelling-wave ansatz into the Herty-Illner macroscopic traffic model are simplified. Both equations (2.1) are rendered more tractable by affine mappings to reduce the number of parameters for a more concise representation (2.9,2.10); somewhat contrary to mathematical tradition we motivate these mappings in the same increments as they were developed.

To begin with, for the jam equation (2.10):

$$\big(V + u(s)\big)^2 u'(s) = -c_1 c_0 V(u(s + H + Tu(s) - \tau V) - u(s))$$

it is no trouble to set $z(s) := u(s) + V$ and $\beta := -c_1 c_0 V$ to derive:

$$\frac{d}{ds}\left(\frac{1}{3}z(s)^3\right) = \beta[z(s + H + Tz(s) - (\tau + T)V) - z(s)]. \tag{2.4}$$

This looks friendlier but we can do better: looking at a simpler abridged version of the equation might help to motivate further developments.

2.2.1 Abridged Jam-Equation

An avenue for exploring the possibility of existence for solutions of the jam equation above is the study of a related (abridged) form (where $\delta := H - (\tau + T)V$) where, relative to (2.4), the factor of $z^2(s)$ has been deleted from the left-hand side:

$$\begin{aligned}\frac{d}{ds}z(s) &= \beta[z(s + H + Tz(s) - (\tau + T)V) - z(s)] \\ &= \beta[z(s + \delta + Tz(s)) - z(s)].\end{aligned} \tag{2.5}$$

2.2.2 Proposition: Transformations (Abridged Jam-Equation)

Supposing $z = z(s)$ is a solution of (2.5) we let:

$$z_1(s) = z(s + \alpha), \quad z_2(s) = \alpha z(s), \quad z_3(s) = z(\alpha s), \quad z_4(s) = z(s) + \alpha.$$

Then we have the following identities:

$$\begin{aligned}
z_1'(s) &= \beta[z_1(s+\delta+Tz_1(s)) - z_1(s)] \\
z_2'(s) &= \beta[z_2(s+\delta+\frac{T}{\alpha}z_2(s)) - z_2(s)] \\
z_3'(s) &= \alpha\beta[z_3(s+\frac{\delta}{\alpha}+\frac{T}{\alpha}z_3(s)) - z_3(s)] \\
z_4'(s) &= \beta[z_4(s+(\delta-\alpha T)+Tz_4(s)) - z_4(s)].
\end{aligned}$$

2.2.3 Proposition: Consequences

Letting $\alpha = \frac{\delta}{T}$ and $\overline{z}(s) = z(s)+\alpha$, we derive: $\overline{z}'(s) = \beta[\overline{z}(s+T\overline{z}(s))-\overline{z}(s)]$. Moreover, letting $\alpha = T$ and $\overline{z}(s) = \alpha z(s)$, we derive: $\overline{z}'(s) = \beta[\overline{z}(s+\overline{z}(s)) - \overline{z}(s)]$. Relabeling this, an equivalent form of (2.5) is demonstrated:

$$z'(s) = \beta[z(s+z(s)) - z(s)]. \tag{2.6}$$

2.2.4 Proposition: Transformations (Jam-Equation)

Cf. (2.4), suppose $z = z(s)$ solves $z^2(s)\frac{d}{ds}z(s) = \beta[z(s+\delta+Tz(s)) - z(s)]$. Let:

$$z_1(s) = z(s+\alpha), \quad z_2(s) \quad = \alpha z(s), \quad z_3(s) = z(\alpha s), \quad z_4(s) \quad = z(s)+\alpha. \tag{2.7}$$

Then we have the following identities:

$$\begin{aligned}
z_1(s)^2 z_1'(s) &= \beta[z_1(s+\delta+Tz_1(s)) - z_1(s)] \\
\frac{1}{\alpha^2}z_2(s)^2 z_2'(s) &= \beta[z_2(s+\delta+\frac{T}{\alpha}z_2(s)) - z_2(s)] \\
z_3(s)^2 z_3'(s) &= \alpha\beta[z_3(s+\frac{\delta}{\alpha}+\frac{T}{\alpha}z_3(s)) - z_3(s)] \\
(z_4(s)-\alpha)^2 z_4'(s) &= \beta[z_4(s+(\delta-\alpha T)+Tz_4(s)) - z_4(s)].
\end{aligned}$$

2.2.5 Proposition: Consequences

As before, let $\alpha = \frac{\delta}{T}$ for $z_4(s)$ and $\alpha = T$ for $z_2(s)$, deriving the equivalent equation (the simplified representation for the braking functional-differential-equation):

$$(z(s)-\alpha)^2 z'(s) = \beta[z(s+z(s)) - z(s)].$$

2.2.6 The Simplified Equations

For the acceleration functional-differential-equation (the un-jam equation):

$$\big(V + u(s)\big)^2 u'(s) = -c_2(\rho_{max}(u(s) + V) - c_0 V)(u(s) - u(s + H + Tu(s) - \tau V))$$

we take, representative of the composition of the motivational maps just considered, the following affine mapping as in [9]:

$$u(s) := \frac{1}{T} z(s) - \delta; \quad \delta := \frac{1}{T}(H - \tau V). \tag{2.8}$$

Then $u'(s) := \frac{1}{T} z'(s)$ and letting $\alpha := T(V - \delta)$, for one term

$$\begin{aligned}
\big(V + u(s)\big)^2 u'(s) &= \big(V + \frac{1}{T} z(s) - \delta\big)^2 \frac{1}{T} z'(s) \\
&= \big(T(V - \delta) + z(s)\big)^2 \frac{1}{T^3} z'(s) \\
&= \big(z(s) + \alpha\big)^2 \frac{1}{T^3} z'(s)
\end{aligned}$$

and the other using also $\gamma := \alpha - \frac{c_0}{\rho_{max}} VT$ and $\beta = c_2 \rho_{max} T$:

$$\begin{aligned}
& c_2(c_0 V - \rho_{max}(u(s) + V))(u(s) - u(s + H + Tu(s) - \tau V)) \\
&= c_2(c_0 V - \rho_{max}(\frac{1}{T} z(s) - \delta + V))(\frac{1}{T} z(s) - \delta - u(s + T(u(s) + \delta))) \\
&= c_2(c_0 V - \rho_{max}(\frac{1}{T} z(s) - \delta + V))(\frac{1}{T} z(s) - \delta - u(s + T(\frac{1}{T} z(s) - \delta + \delta))) \\
&= c_2(c_0 V - \rho_{max}(\frac{1}{T} z(s) - \delta + V))(\frac{1}{T} z(s) - \delta - (\frac{1}{T} z(s + z(s)) - \delta)) \\
&= c_2(c_0 V - \rho_{max}(\frac{1}{T} z(s) - (\delta - V))(\frac{1}{T} z(s) - \frac{1}{T} z(s + z(s))) \\
&= \frac{c_2}{T^2}(c_0 VT - \rho_{max}(z(s) + \alpha))(z(s) - z(s + z(s))) \\
&= \frac{c_2 \rho_{max}}{T^2}(\frac{c_0}{\rho_{max}} VT - (z(s) + \alpha))(z(s) - z(s + z(s))) \\
&= -\frac{\beta}{T^3}(z(s) + \gamma)(z(s) - z(s + z(s))) \\
&= \frac{\beta}{T^3}(z(s) + \gamma)(z(s + z(s)) - z(s)).
\end{aligned}$$

Finally to derive the **simplified un-jam equation** we collect the terms:

$$\big(z(s)+\alpha\big)^2 z'(s) = \beta(z(s)+\gamma)(z(s+z(s))-z(s)). \tag{2.9}$$

where we have the new definitions $\beta := c_2\rho_{max}T$, and $\gamma := \alpha - \frac{c_0}{\rho_{max}}VT$. As in [9] using also (2.8) the **simplified jam-equation** is:

$$\big(z(s)+\alpha\big)^2 z'(s) = \beta(z(s+z(s))-z(s)) \tag{2.10}$$

with the new definition $\beta := c_0c_1VT^2$. In both cases (2.9,2.10) we have the new definitions $\alpha := T(V-\delta)$ and $\delta := \frac{1}{T}(H-\tau V)$.

In conclusion, the **simplified un-jam equation** (2.9) and the **simplified jam-equation** (2.10) are functional equations equivalent to (but algebraically simpler than) the original functional equations: the **jam equation** (1.50) and the **unjam equation** (1.52), respectively. The "simplified" equations (2.9,2.10) are both related to (1.50,1.52) by the same affine transformation (2.8).

2.3 Challenges And Open Problems

2.3.1 Challenges Due To Transformed Arguments

Equations simpler than those **iterated-functional-differential-equations** arising from the macroscopic traffic model, for example the **differential-delay-equations**, are worthwhile to mention for illustration of some of the challenges involved, before revisiting the more general **iterated-functional-differential-equations** (2.1) derived from the Herty-Illner model.

One delay: Cauchy-Monge Ansatz

The Cauchy-Monge Ansatz $x(t) = ce^{\lambda t}$ applies to the following **linear differential-delay-equation** in $x(t)$, $r \in \mathbb{R}$ (the delay) being some (known) parameter:

$$\dot{x}(t) = Ax(t) + Bx(t-r). \tag{2.11}$$

Specifically,

$$c\lambda e^{\lambda t} = cAe^{\lambda t} + cBe^{\lambda(t-r)}$$

i.e., $x(t) = ce^{\lambda t}$ solves (2.11) for λ such that

$$\lambda - A - Be^{-\lambda r} = 0. \tag{2.12}$$

The equation (2.11) is none other than the following linear abridged version of the jam-equation considered by Illner and MacGregor [9]:

$$z'(s) = \beta[z(s + z_0) - z(s)] \tag{2.13}$$

where, relative to (2.10), the factor $(z(s) + \alpha)^2$ is omitted from the left-hand side. Furthermore, the non-local dependency $z(s+z(s))$ is replaced by the simpler non-local dependency $z(s + z_0)$ which represents a shift of $z(s)$ with respect to some constant factor z_0 (rather than a shift of $z(s)$ with respect to itself).

To illustrate some flavours exhibited by equations where the transformations are more exotic, we can consider the same example with an additional delay:

Multiple delays: Higher-dimensional parameterization

Equations with multiple delays, e.g. the **difference equation**

$$x(t) = Ax(t - 1) + Bx(t - 2) \tag{2.14}$$

may be treated by expressing (2.14) via $y(t) = x(t - 1)$ as:

$$z(t) = Cz(t - 1) \tag{2.15}$$

where $z = \begin{bmatrix} x \\ y \end{bmatrix}$ and $C = \begin{bmatrix} A & B \\ 1 & 0 \end{bmatrix}$. The solution on $[t, \infty)$ is [6]:

$$z(t) = C^{t-\theta}\phi(\theta) \tag{2.16}$$

where $\theta = t - \lfloor t \rfloor - 1 \in [-1, 0]$ and $\phi(\theta) : [-1, 0] \to \mathbb{R}^2$ is arbitrary.[2] Thus the solution is described in terms of a linear transformation on $\mathbb{R}^2$.

The example (2.16) highlights some unusual and persistent features of equations with transformed arguments which follow.

[2]Hale [6] also notes the possibility of taking the exponential ansatz $x(t) = c\lambda^t$ $(c \neq 0)$ in (2.14) from which a characteristic equation may be derived (the roots of which are, in fact, the eigenvalues of C).

- There is a **non-local** "memory-like" effect: the solution exhibits non-local reference to values it takes elsewhere[3].
- The solution might depend upon some arbitrary (undetermined) "initial data", e.g. $\phi(\theta)$ for (2.16).

It is worth mentioning that the iterated-functional-differential-equations of interest: the jam and un-jam equations, might be expressed as a higher-dimensional system of (local) differential-equations: however the resulting system would be both nonlinear as well as infinite-dimensional.

For the jam-equation and related equations it is simple to observe the difficult **non-local** relationships involved: supposing the derivatives exist, a simple repeated application of differentiation (one step shown here for (2.6)):

$$z'(s) = \beta[z(s + z(s)) - z(s)]$$
$$z''(s) = \beta[z'(s + z(s))(1 + z'(s)) - z'(s)]$$

reveals that the higher derivatives depend upon lower derivatives evaluated elsewhere.

2.3.2 Challenges Due To Iteration

Above and beyond the non-local, possibly high dimensional, and memory-like nature of delay equations, and even the possible dependence upon arbitrary (undetermined) functions, our examples provide other challenges. The established analytic (series) solution methods [8] for iterated-functional-differential-equations, possibly the simplest being:

$$x'(s) = x(x(s)) \tag{2.17}$$

are based on two steps, as follows:

1. substitution of the ansatz $x(s) = y(\mu y^{-1}(s))$, and,
2. formal power series coefficient determination for $y(s)$.

[3]For (2.9,2.10) the implied dependence of the derivatives of the solution upon $z(s+z(s))$ suggests to us that the values taken by the solution could be "repeated" according to some non-local pattern. Indeed, the example (2.16) shows a system with (two) multiple delays exhibiting a "repeated" solution. Effectively, there are also multiple delays inherent in the equations (2.9,2.10); since these delays are (potentially) infinite in number the situation is more complicated.

The operation representative of $x(s) = g(\mu g^{-1}(s))$ is referred to as the **Schröder transformation.** For (2.17) the identities (2.18,2.19):

$$\begin{aligned} x(x(s)) &= g(\mu g^{-1}(g(\mu g^{-1}(s)))) \\ &= g(\mu g^{-1} \circ g(\mu g^{-1}(s))) \\ &= g(\mu^2 g^{-1}(s)) \end{aligned} \tag{2.18}$$

$$\begin{aligned} x'(s) &= (g(\mu g^{-1}(s)))' \\ &= \mu \frac{g'(\mu g^{-1}(s))}{g'(g^{-1}(s))} \end{aligned} \tag{2.19}$$

lend (2.17) an alternative representation:

$$\mu g'(\mu g^{-1}(s)) = g(\mu^2 g^{-1}(s)) g'(g^{-1}(s)).$$

Letting $z := g^{-1}(s)$ simplifies the above further:

$$g'(\mu z) = \frac{1}{\mu} g'(z) \cdot g(\mu^2 z). \tag{2.20}$$

The last equation is referred to as an **auxilliary equation** for (2.17): this transformed representation of (2.17) is an equation in $y(s)$ of a form amenable to analytic series coefficient determination. Considering which $\mu \in \mathbb{R}$ might be admissible is a nontrivial matter [8]. The success of the method depends on demonstrating:

- the convergence of the power series for $y(s)$ (argued by majorization) and that,
- the solution $x(s) = y(\mu y^{-1}(s))$ determined by these coefficients is in fact a solution.

Discussion

In applying the above analytic expansion methods [8] to the jam and un-jam equations, it can be seen that the series for the associated auxilliary equations cf. (2.20) are divergent. The partial development of a fascinating alternative operator approach is the subject of [9]. Furthermore the methods of [8] are applied successfully to the jam equation in [35] for a case other than that considered here: namely the case

of solutions passing through the origin (for the jam equation, the desired solutions associated with the travelling wave profile should be non-negative, monotonically decreasing, and of infinite support). Despite these advances the answer to the existence question for the jam and un-jam equations remains outstanding: thus the existence riddle is representative of an open problem of great intrigue and difficulty.

Chapter 3

Non-Local Driving Behaviour with Fundamental Diagrams

The macroscopic model [3] presented here extends the macroscopic traffic models of Herty and Illner [1, 2] by augmenting and reconciling the usual non-local forces representative of interactive driver behaviour with relaxation terms (representative of free-flow dynamics). Again, relative to [1] the modelling also includes the addition of the reaction time parameter τ which we should expect, is observed in practice, and which forces us to pay close attention to the range of validity for the models.

First the refined macroscopic model [3] is developed: in addition to the usual non-local forces, the refined model includes a relaxation term. Subsequent to these developments, the behaviour of the refined model is exhibited through numerical simulations, where emphasis is placed upon the question of stop-and-go wave formation[1].

Throughout the interpretation of macroscopic variables described before (1.1.3) is assumed.

3.1 Motivation

The non-local Herty-Illner traffic models [1, 2] which were derived from Vlasov-type kinetic (mesoscopic) models and shown to admit (at least approximately) travelling wave solutions [1, 2] were known to obey maximum principles [2]. The interpretation of the maximum principles is that the traffic dynamics are not self-excitatory. The desired self-excitation may follow from a relaxation term (based on a fundamental

[1]The answer to this question is affirmative.

diagram) like the "relaxation" type of force terms typically incorporated in models of Aw-Rascle-Zhang type [36]. That is, the relaxation term (representative of the propensity to "return to an equilibrium state") is necessitated by the assumption that drivers will adjust their speed to some ideal (comfortable) "target speed" $U^e(\rho)$, in the absence of more pressing behavioural stimuli (e.g., braking or acceleration events ahead that invite the driver to respond in anticipation of the future state).

It is assumed that the "target speed" involved in the relaxation term will be represented by a fundamental diagram. Formally speaking, a fundamental diagram is a relationship between traffic flux (often expressed in units of vehicles/hour) and the traffic density (often expressed in units of vehicles/km) which is usually an empirically determined relationship (perhaps obtained by curve fitting to real traffic data). In the macroscopic modelling context we shall also use the term "fundamental diagram" to refer to an (equivalent) relationship between traffic speed u (instead of traffic flux ρu) and traffic density ρ. The fundamental diagrams used here to represent the "target speed" in the relaxation term will be, rather than empirically derived curves, idealized curves familiar to the traffic modelling community for the same purpose.

The observation [1] that the models cf. [2] formally admit steady (constant) solutions (ρ, u) for (arbitrary) density and speed combinations emphasizes that the inclusion of a relaxation term is of great importance, particularly for high-density situations.

3.1.1 Relaxation Terms

Relaxation terms, typically included in second-order macroscopic traffic models on the right hand side of the usual momentum-transfer equation, are usually[2] representative of acceleration (deceleration) towards a comfortable (equilibrium) target speed $U^e(\rho)$.

Conventionally the target speed $U^e(\rho)$ is assumed to be density-dependent. The most prominent example of a density-dependent relaxation term is:

$$\frac{1}{T_0}(U^e(\rho) - u) \tag{3.1}$$

where T_0 is the so-called characteristic relaxation time, that is, drivers adjust their speed u according to the discrepancy $(U^e(\rho) - u)$ with the ideal speed. The proportion $\frac{1}{T_0}$ is chosen so that, according to the instantaneous (linear) forecast, the discrepancy

[2] A relaxation term could also take into account the activity of speed limits or other laws, although here speed limits will be considered "separately" in (3.3.4).

$(U^e(\rho) - u)$ will be resolved (tend to zero) at at time T_0 from now[3] (in the modelling that follows, the quantity $\frac{1}{T_0}$ will be referred to as c_3). Equation (3.1) has dimensions of acceleration (or braking).

Models of Aw-Rascle-Zhang type have been studied with right hand sides corresponding to $U^e(\rho)$ represented by a variety of fundamental diagrams [24, 37, 36]. Of particular interest is the emergence of three-phase traffic dynamics (cf. Kerner [38]) consequent to the assumption of a multi-valued fundamental diagram [36]. As in [36] a multi-valued fundamental diagram is considered here, to augment the non-local macroscopic traffic models introduced in [1, 2].

There are many types of models other than those developed here, as noted in Chapter (1). Some aspects left out of the modelling so far include but are not limited to the following: variations in vehicle size and mass, individual driver behaviour, and random fluctuations. Here priority is given to simplicity, in order to identify basic structures as those indicated by empirical studies, for example those identified by three-phase traffic theory.

Again (1.1.3), while the macroscopic models here are developed from the Fokker–Planck ansatz cf. [20, 1, 39, 16], the subject of macroscopic modelling has been subject to intensive study eg. [4, 40, 41, 42, 37, 26, 43, 44, 28, 29, 5, 45, 46]. On the other hand, microscopic models keeping track of individual drivers and their interactions (as systems of ordinary differential-delay equations, or discrete versions like cellular automata) have also been subject to intense study [47, 48, 49, 50, 38, 51, 52, 53]; stochastic extensions of these models are also available [54, 55, 56]. Lastly the kinetic models, see e.g. [18], represent the bridge between the microscopic and macroscopic perspectives.

3.2 Modelling

3.2.1 Parameters and Notation

As before (1.1.3), position (on the road) and time will be denoted by x, t. The symbols

$$\rho = \rho(x,t), u = u(x,t)$$

[3]Of course, it is only an instantaneous (forecast) so the time T_0 for resolution of the discrepancy is an idealized estimate. Further, the estimate is based on an idealized driver that does not take other drivers' speeds into account, i.e., the estimate does not include the effects of possible fluctuations in the speed profile.

refer, respectively, to the macroscopic density and the macroscopic (average) speed of cars on a highway (freeway) lane. Lane changing is not given explicit consideration here, although it may be included implicitly in the sense that certain types of fundamental diagrams (to be introduced later) emerge only due to the presence of lane-changing. The non-local model includes three parameters that exist in real traffic:

- **the minimum safety distance** $H > 0$ (on the order of magnitude of 8 meters and measured from the front of a car to the front of the lead car) which applies in moving traffic and is larger than the minimum distance in standing traffic, i.e., $\frac{1}{\rho_{\max}}$;
- **a characteristic reaction time** $T > 0$ that multiplies the driver's speed such that: $[x, x + H + Tu]$ is the window from which a driver at x and moving with speed u draws (visual) information;
- **the individual driver reaction time** $\tau > 0$. T should be thought of as being about 2 seconds, $\tau \approx 1$ second.

At a typical speed of 15 meters per second, the window $[x, x + H + Tu]$ would then be 38 meters long.

With u, ρ taken at (x, t) the following abbreviations are introduced:

$$u^X(x,t) = \inf_{\sigma \in [x, x+H+Tu]} u(\sigma, t-\tau), \tag{3.2}$$

(the smallest speed observed in the visible window)

$$\rho^+(x,t) = \sup_{\sigma \in [x, x+H+Tu]} \rho(\sigma, t-\tau), \tag{3.3}$$

$$u^Y(x,t) = \sup_{\sigma \in [x, x+H+Tu]} u(\sigma, t-\tau), \tag{3.4}$$

and

$$\rho^-(x,t) = \inf_{\sigma \in [x, x+H+Tu]} \rho(\sigma, t-\tau). \tag{3.5}$$

3.2.2 The Fundamental Diagram. Braking and Acceleration Forces

In the absence of speed limits (or other laws) that will be given separate attention later (3.3.4), drivers are assumed to have a target speed in mind associated with a certain density, and if no other inputs are active, they will brake or accelerate towards this target speed. We assert that this behaviour is a certain force F given by a fundamental diagram. In the simplest case F might be taken as:

$$F = \frac{1}{T_0}\left(U^e(\rho) - u\right). \tag{3.6}$$

Again, in the statement of the refined version of the Herty-Illner model (3.14,3.15), the quantity $\frac{1}{T_0}$ will be referred to as c_3.

As indicated earlier, the fact that U^e may be a multi-valued function might best be expressed in terms of a dependence on two variables, rather than one, i.e.,

$$U^e = U^e(\rho, u).$$

Such an example will be provided and used below; the structure of a multi-valued U^e is best understood from a graphical representation (see Fig. 3.1).

We emphasize that the fundamental diagram should be active only if no other (overriding) forces apply. Such forces are active if the driver is in a "compelling" braking or acceleration situation. The word "compelling" here means that the driver realizes the need to brake or accelerate; to this end we introduce one more parameter $\epsilon \geq 0$, a (low) threshold for reaction. The conditions defining braking scenarios, along with the associated force terms to be active on the right hand side of the speed (or momentum transfer) equation, are given by (3.7,3.8):

$$\text{If } \; u - u^X > \epsilon \;\; \text{ let } \;\; B = \min\{c_1 \left(\frac{\rho_{max}\rho^+}{\rho_{max} - \rho^+}\right)(u^X - u), F\}. \tag{3.7}$$

We see that (3.7) means that braking dominates, and the braking force is the stronger of the two given by the speed relative to u^X and the one given by the fundamental diagram. The factor multiplying $u^X - u$ is called "speed adaptation coefficient" (see [36] and associated references), which diverges to ∞ as ρ^+ approaches the possible maximum.

$$\text{If } \; u - u^X \leq \epsilon \;\; \text{ and } \;\; F < 0 \;\; \text{ let } \;\; B = F. \tag{3.8}$$

This means that braking still dominates (drivers are 'compelled" to brake) if the fundamental diagram calls for braking, even if the relative speed is close to 0 or negative.

Next the condition (3.9) is provided to define the acceleration scenario, along with the associated force term (3.10) active on the right hand side of the speed (or momentum transfer) equation:

$$\text{If } \; u - u^X \leq \epsilon, \; F \geq 0 \; \text{ and } \; u^Y - u > \epsilon \tag{3.9}$$

let the acceleration force A be defined by:

$$A = \max\{c_2(\rho_{max} - \rho^-)(u^Y - u), F\}. \tag{3.10}$$

This is an acceleration scenario, for which acceleration is given either by the force suggested by the speed relative to u^Y, or by the fundamental diagram. As the speed adaptation coefficient is taken here to be a function decreasing with ρ^- – higher densities should imply reduced acceleration. Finally, if none of the above conditions (3.7,3.8, 3.9) apply, the force is simply F – the fundamental diagram is the only remaining input.

In the following numerical simulations we allow different fundamental diagrams as depicted in Figure 3.1 and explained in detail below.

I) The Greenshields model with two parameters (maximal velocity $v_{\max}$ and maximal density $\rho_{\max}$) is given by:

$$U^{eq}(\rho) = v_{\max}(\rho - \rho_{\max}). \tag{3.11}$$

II) A more realistic nonlinear fundamental diagram is:

$$U^e(\rho) = v_{\max}\left(1 - \frac{1}{\pi}\left(atan\left(30\pi\left(\rho - \frac{\rho_{\max}}{3}\right)\right) + \frac{\pi}{2}\right)\right). \tag{3.12}$$

The shape of this fundamental diagram is similar to the examples considered in [18]. It is a better match to traffic data due to the small transition zone between free flow ($\rho < \frac{\rho_{\max}}{3}$) and congested traffic.

III) An example of fundamental diagram attaining multiple values in the region $I := [\rho_-, \rho_+]$ given by:

$$U^e(\rho,u) = \begin{pmatrix} U^e\left(\rho + \frac{\rho_{\max}}{3} - \frac{5}{4}\rho_+\right) & u > u^*(\rho), \rho \in I \text{ or } \rho < \rho_- \\ u^*(\rho) & u = u^*(\rho), \rho \in I \\ U^e\left(\rho + \frac{\rho_{\max}}{3} - \frac{3}{4}\rho_-\right) & u < u^*(\rho), \rho \in I \text{ or } \rho > \rho_+ \end{pmatrix} \tag{3.13}$$

where is $U^e(\rho)$ is chosen to be as given by (3.12). The other parameters are as follows: $\rho_\pm = \frac{\rho_{\max}}{3} \pm \frac{1}{20}\rho_{\max}$, $u^*(\rho) = \frac{u_+ - u_-}{\rho_+ - \rho_-}(\rho - \rho_-) + u_-$ for $u_- = U^e(\frac{1}{2}\rho_-)$ and $u_+ = U^e(-\frac{1}{4}\rho_-)$. Similar fundamental diagrams were used in [36] to show how multi–valued fundamental diagrams help explain stop–and–go waves.

The above fundamental diagrams are depicted in Figure (3.1) where the equilibrium speeds are given by the dotted red lines. The contours for the velocities $U_e(\rho,u) - u$ corresponding respectively to the acting forces derived from $U_e(\rho,u)$ are represented in "heat map" format, i.e., in the (ρ,u) plane, the velocities $U_e(\rho,u) - u$ are indicated by color. For each of the diagrams represented in Figure (3.1) the correspondence between color and velocity is shown via the "thermometer" scale at the right. Then, negative velocities $U_e(\rho,u) - u$ are representative of braking, whereas positive velocities $U_e(\rho,u) - u$ are representative of acceleration.

These definitions define forces for all possible scenarios as a functional of the (delayed, non-local) state. Writing R for this functional, the traffic model is:

$$\rho_t + (\rho u)_x = 0 \tag{3.14}$$

$$u_t + u u_x = R. \tag{3.15}$$

Notice that the B which arises in braking scenarios is by construction always nonpositive. The definition of the force term R is asymmetric in preference of braking, a reasonable construction in view of safety considerations.

3.3 Numerical simulations

The System In Conservative Form

In order to proceed with numerically solving the system of balance laws (3.14-3.15), the momentum equation (3.15) is rewritten in terms of the conservative variable (ρu)

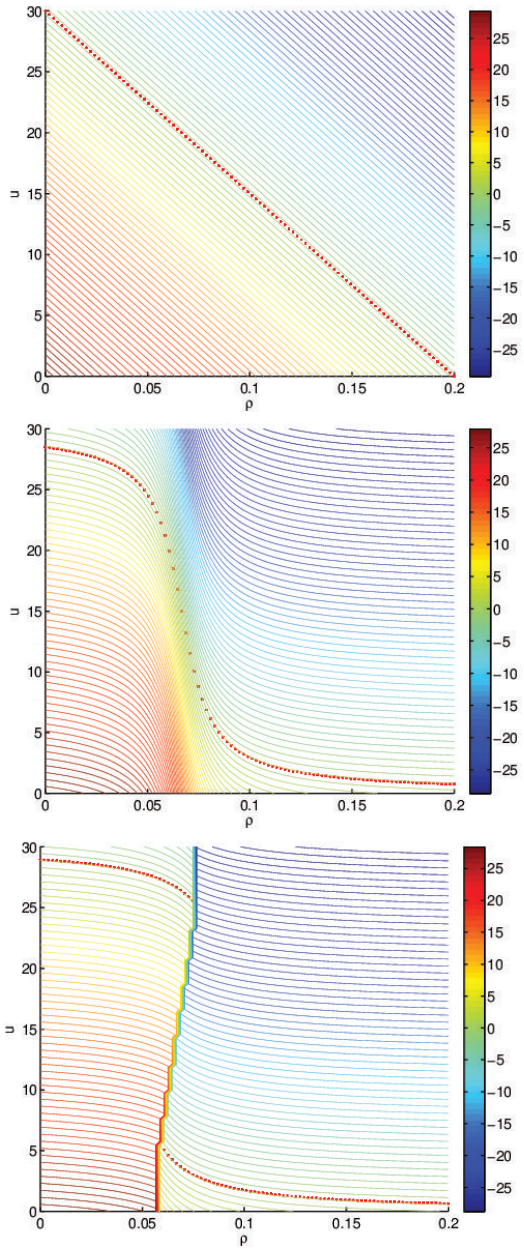

Figure 3.1: Equilibrium velocities $U^e, U^e(\rho, u)$ (dotted red line) resp. given by (3.11)-(3.13). Also shown: the contour lines of the relative velocities: $U^e(\rho, u) - u$ from which the acting forces are derived.

to obtain the system

$$\begin{aligned} \rho_t + (\rho u)_x &= 0 \\ (\rho u)_t + (\rho u^2)_x &= \rho R. \end{aligned} \tag{3.16}$$

We see this by rewriting (3.14) as (3.17):

$$\begin{aligned} 0 &= \rho_t + (\rho u)_x \\ &= \rho_t u + \rho_x u^2 + \rho u_x u. \end{aligned} \tag{3.17}$$

Inserting (3.17) into the product of (3.15) with ρ: $\rho(u_t + uu_x - R) = 0$, yields the equivalent momentum law (3.18):

$$\begin{aligned} \rho R &= \rho u_t + \rho u u_x + \rho_t u + \rho_x u^2 + \rho u u_x \\ &= (\rho u)_t + (\rho u^2)_x \end{aligned} \tag{3.18}$$

as desired cf. (3.16).

Numerical Solution Via The Conservative Form

The numerical solution for (3.16) computed on a uniform grid with N_x spatial grid points is obtained using a first–order time–splitting procedure. Specifically, an iteration of the time–splitting procedure consists of the following two steps: 1) the application of a first–order finite volume method, representative of the numerical solution of the system of conservation laws

$$\begin{aligned} \rho_t + (\rho u)_x &= 0 \\ (\rho u)_t + (\rho u^2)_x &= 0 \end{aligned} \tag{3.19}$$

and 2) the application of the Euler method[4] upon the associated ordinary differential equation:

$$(\rho u)_t = \rho R. \tag{3.20}$$

[4]We note that the time step for the Euler method used to numerically solve the ordinary differential equation (3.20) is chosen to satisfy the associated Courant-Friedrichs-Lewy (CFL) condition.

Moreover, the transport system (3.19) corresponds to the well–known equations of pressure-less gas dynamics, for which a Godunov scheme (first–order finite volume method) in the conservative variables $(\rho, \rho u)$ is available [10] – the same method is used here. The interested reader may examine [57] for references to alternative discretization schemes.

Before proceeding to the simulation results, we present the implementation details, as follows. Evaluation of the source term R is performed at the center of each cell; the variables ρ and u are represented as piecewise constant in their reconstruction. For the computation of the non-local term u^X nearest-neighbor interpolation is used. Unless stated otherwise, periodic boundary conditions are used, representative of a circular "ring" road). Parameter values are taken as in Table (3.1). Prescription of the initial data for the simulations will be discussed shortly.

3.3.1 Parameters

The source term R in the equation (3.15) contains the following parameters. The safety distance (H) is taken to be about twice the car length, so that the maximal density is $\rho_{\max} = 0.2$ (corresponding to an average car length of five metres). The anticipation time of the drivers (T) is two seconds which at maximal velocity corresponds to an additional look-ahead distance of 60 m. The maximal velocity ($u_{\max}$) is set to 108 km/h — a model for highway traffic in the USA and Canada. The following possible reaction times (τ) for drivers were simulated: $\tau = 0, \frac{1}{2}, \frac{1}{2}, \frac{3}{4}$ seconds. The weights c_1, c_2, c_3 for braking, acceleration and free flow traffic are a–priori unknown, but we assume that the drivers have a tendency to apply a braking force of greater magnitude than that of a force arising from acceleration behaviour and/or response to free-flow. Traffic is simulated for twenty second periods on a strip of the highway which is four kilometres in length. The mesh consists of 20,000 points (one grid point per twenty centimetres). Table 3.1 summarizes the parameters.

The initial data are described case by case for each of the three traffic scenarios which follow.

Name	Description	Value	Unit
H	safety distance	10	m
T	anticipation time	2	s
$\rho_{\max}$	maximal density	0.2	$1/m$
$u_{\max}$	maximal velocity	30	m/s
τ	reaction time	$\in \{0, \frac{1}{4}, \frac{1}{2}, \frac{3}{4}\}$	s
c_1	weight (braking)	16	$1/s$
c_2	weight (acceleration)	3	$1/s$
$c_3 \equiv \frac{1}{T_0}$	weight (equilibrium)	0.05	$1/(ms)$
ϵ	velocity threshold	0.15	m/s
$L_{\max}$	length of the road	4'000	m
L_{res}	length of speed limit	200	m
u_{lim}	speed limit velocity	15	m/s
$T_{\max}$	time horizon of the simulation	20	s
N_x	gridpoints in spatial domain	20'000	

Table 3.1: Parameters of the numerical simulations

Discussion

3.3.2 Time evolution of a density blip

Similar to that of [2, Section 4.2.1] the first experiment is concerned with the situation where density is assumed to take the constant value $\rho_0 = \frac{1}{5}\rho_{\max}$ on all points but those on a window of length $400m$ centred at $x = 2000m$. The points on this window are subject to the following perturbation: within the window the initial density is prescribed to be smoothly increasing from $\frac{1}{5}\rho_{\max}$ to approximately $\frac{1}{2}\rho_{\max}$ followed by the corresponding decay back to $\frac{1}{5}\rho_{\max}$. An initially constant velocity $u_0 = U^e(\rho_0)$ is prescribed for the *whole* spatial interval (represented in Figure (3.2) by the solid lines in the velocity profile at the right). The scenario represents a situation where higher density has developed at some point of the road (owing to some suddenly occurring traffic disturbance) which at time $t = 0$ has not yet been recognized by drivers upstream. Imminently such recognition will occur, and drivers' reactions will ensue. Several experiments were performed, as follows.

In Figure (3.2) we present density and velocity at a time $T_{\max}$ using the three different fundamental diagrams in the simulation, with the reaction times: 0, $\tau = \frac{1}{4}$,$\tau = \frac{1}{2}$. Figure (3.3) presents a close-up of the same results as (3.2) using the same three reaction times τ as in (3.2) but using only the latter two fundamental diagrams (3.12,3.13) respectively shown in blue and black.

The different initial velocities are due to the fact that the fundamental diagrams (3.11)-(3.13) gives different u_0 associated with ρ_0. The maximal velocity is the same in all simulations. We observe at the bottom of Figure 3.3 the occurrence of oscillations representative of stop–and–go waves. For both fundamental diagrams (3.12) and (3.13) the wavelength is between 50 m and 100 m, which is in good agreement with traffic observations. The staircase-like structure observed in the speed profiles results from the non-locality in u. The size of the "steps" is related to H and T; thus for $H = T = 0$ they would disappear.

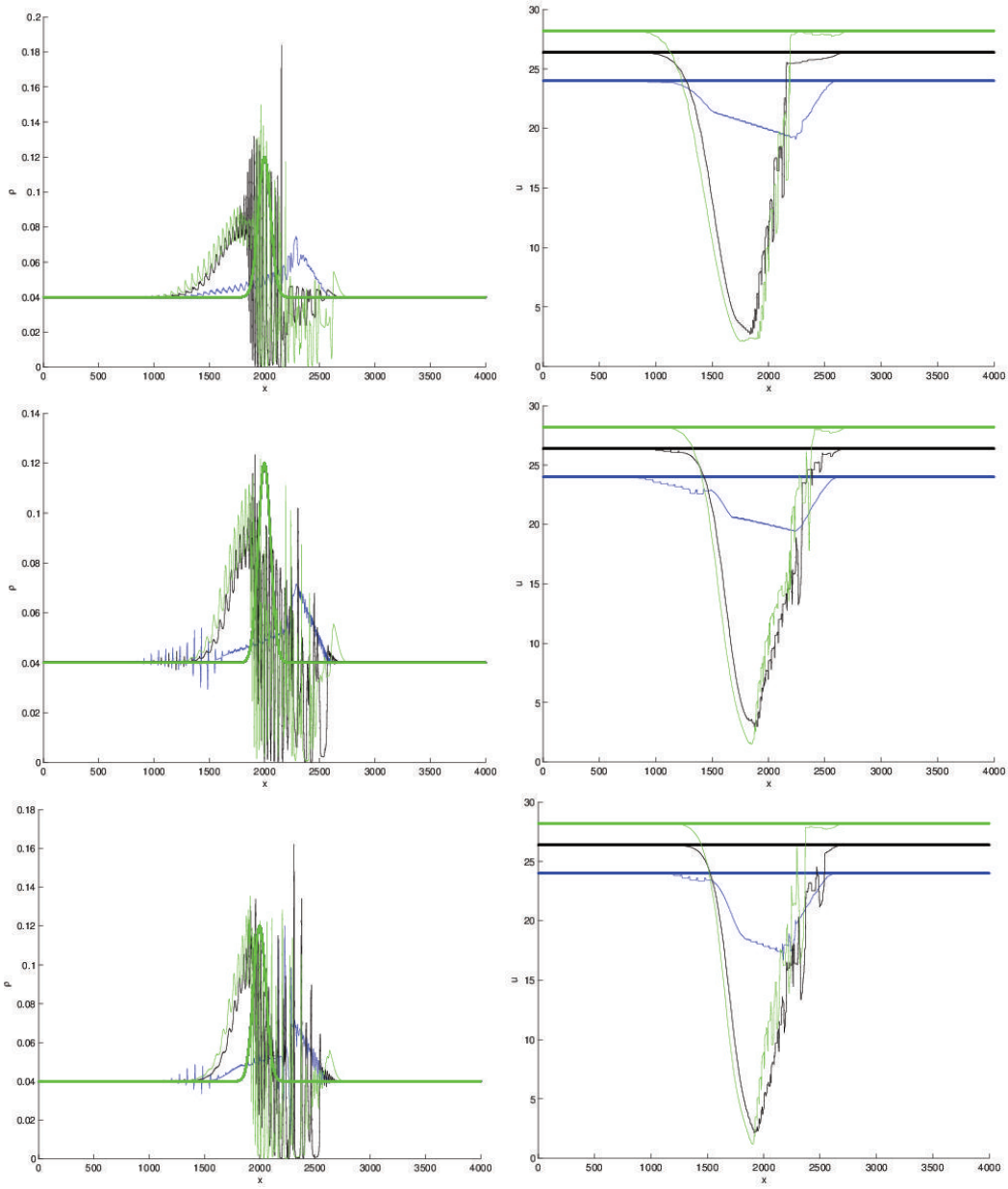

Figure 3.2: Density and velocity at time $T_{\max}$ for initial data having a suddenly increased value of the density and constant initial velocity. Different colors correspond to the different fundamental diagrams used in the simulation: blue, black and green correspond resp. to (3.11), (3.12) and (3.13). The reaction times are $\tau = 0$ (top row), $\tau = \frac{1}{4}$ (middle row), $\tau = \frac{1}{2}$ (bottom row). Left: density, right: velocity.

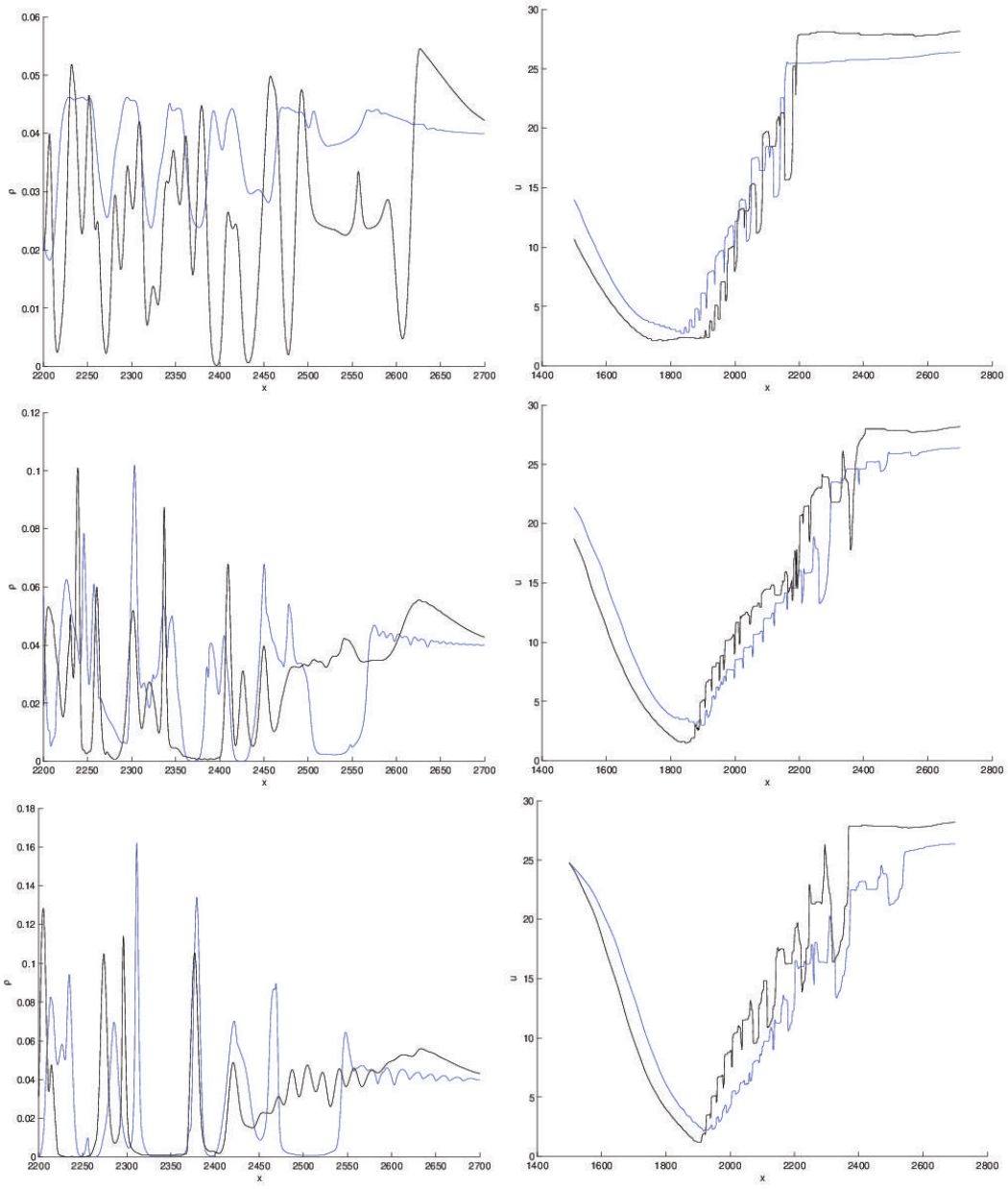

Figure 3.3: Density and velocity at time $T_{\max}$ for initial data having a suddenly increased value of the density and constant initial velocity. Different colors correspond resp. to the different fundamental diagrams used in the simulation: blue to (3.12) and black to (3.13). The reaction times are $\tau = 0$ (top row), $\tau = \frac{1}{4}$ (middle row), $\tau = \frac{1}{2}$ (bottom row). Left: density, right: velocity.

3.3.3 The effect of a lane reduction

Next the effect of a lane reduction on the evolution of traffic flow is studied. The lane reduction is modelled by increasing the initially constant density of $\rho_0 = \frac{1}{5}\rho_{\max}$ to $\frac{3}{10}\rho_{\max}$ on a strip centered at $x = 2000m$ whose length is 50% of the road. The initial transition from the lower to higher density is smooth. The transition from higher density back to lower density is also smooth: this represents the exit–point of the lane reduction area. The transition at the exit–point is not the emphasis of this study, but is advantageous in that the circular boundary conditions are respected. The initial velocity is always the equilibrium velocity corresponding to the lower density. Hence the initial conditions represent the situation where cars within the lane reduction area are moving uncomfortably fast (according to the fundamental diagram) hence they react by braking. Due to the length of the lane reduction area, the acceleration effects at the exit–point do not interact with the braking affects associated with the lane reduction.

In Figure (3.4) density and velocity profiles at time $T_{\max}$ are presented, using different fundamental diagrams in the simulation, and the following reaction times: $\tau = 0$ (top row), $\tau = \frac{1}{4}$ (middle row) ,$\tau = \frac{1}{2}$ (bottom row) . This time only the fundamental diagrams corresponding to equations (3.12) and (3.13) are represented (in blue and black, respectively). In Figure (3.5) the same profiles as in Figure (3.4) are shown with zoom, giving a detailed view of the transition at the start of the lane reduction area. Finally, Figure (3.6) shows a contour plot of the full solution over space and time for the fundamental diagram (3.13) using the same reaction times: $\tau = 0$ (top row), $\tau = \frac{1}{4}$ (middle row), $\tau = \frac{1}{2}$ (bottom row).

As before, finite oscillations are seen in the density – these are expected and do not reach or exceed the maximal density in the simulation. The pressure–less gas dynamics model guarantees that changes in the velocity profile will lead to the emergence of density oscillations. The frequency of this oscillations is related to the non-locality in the model. In particular, in Figure (3.5) stop–and–go waves with wavelength of approximately 50 m are observed.

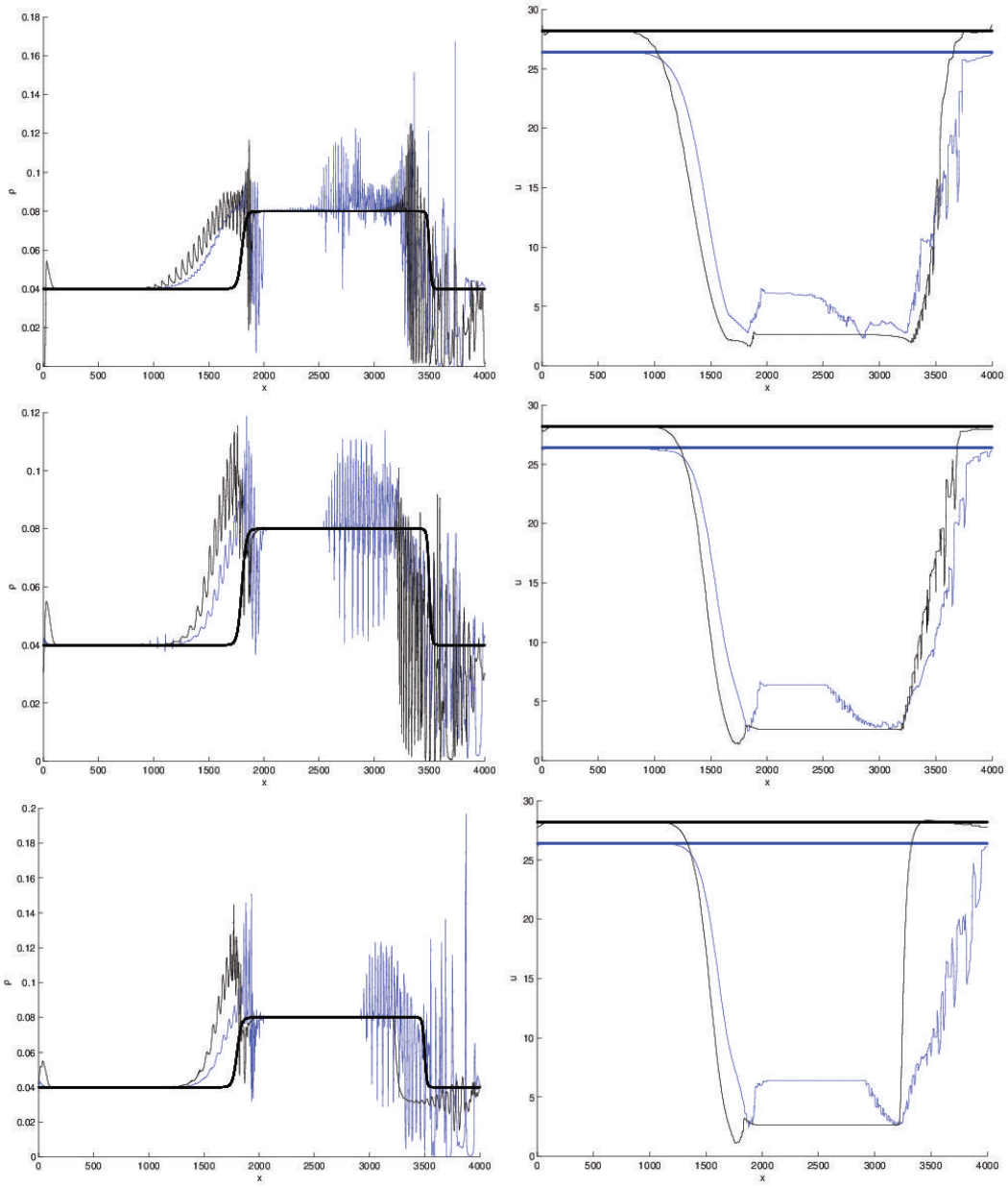

Figure 3.4: Density and velocity at time $T_{\max}$ for initial data corresponding to a lane reduction and constant initial velocity. Different colors correspond resp. to the different fundamental diagrams used in the simulation: blue and black resp. correspond to (3.12) and (3.13). The reaction times are $\tau = 0$ (top row), $\tau = \frac{1}{4}$ (middle row), and $\tau = \frac{1}{2}$ (bottom row). Left: density, right: velocity.

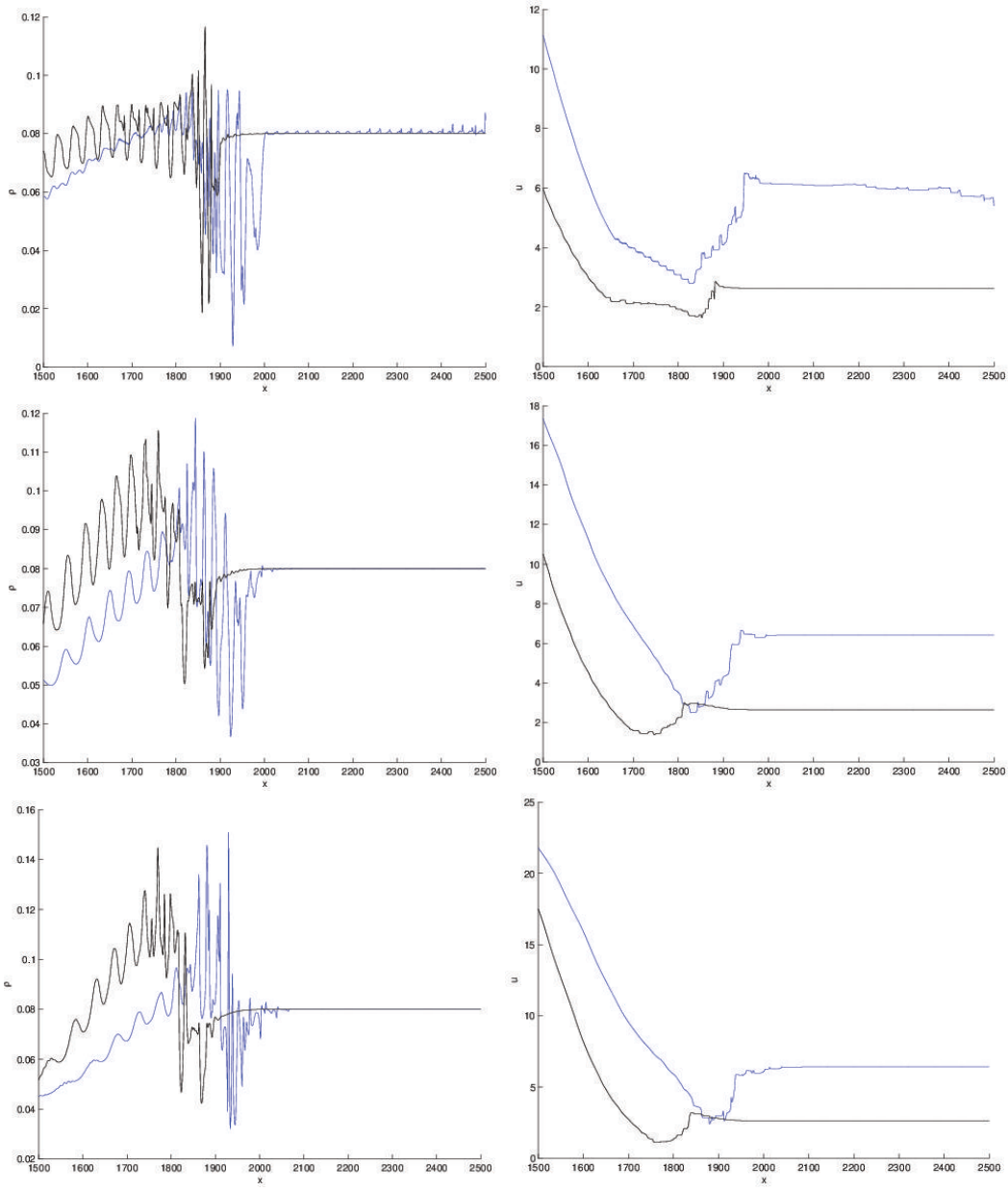

Figure 3.5: Density and velocity at time $T_{\max}$ for initial data corresponding to a lane reduction and constant initial velocity. Different colors correspond resp. to the different fundamental diagrams used in the simulation: blue and black correspond resp. to (3.12) and (3.13). The reaction times are $\tau = 0$ (top row), $\tau = \frac{1}{4}$ (middle row), $\tau = \frac{1}{2}$ (bottom row). Left: density, right: velocity.

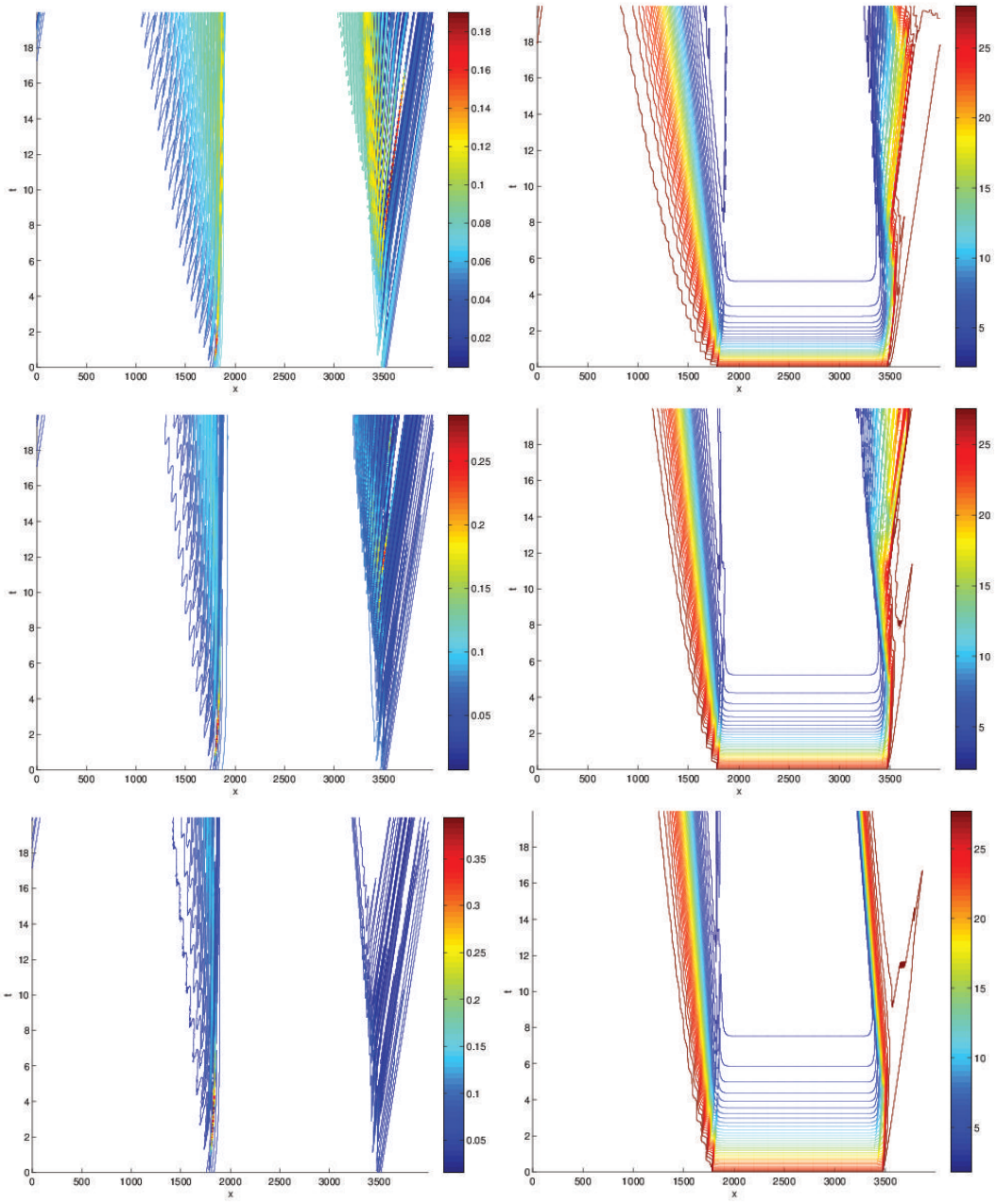

Figure 3.6: Density and velocity contours representing the simulation at times $t \in [0, T_{\max}]$ for initial data corresponding to a lane reduction and constant initial velocity. The fundamental diagram (3.13) is used with the reaction times: $\tau = 0$ (top row), $\tau = \frac{1}{4}$ (middle row), $\tau = \frac{1}{2}$ (bottom row). Left: density, right: velocity.

3.3.4 The effect of a speed limit

Lastly a speed limit scenario is considered, similar to that in [2]: the same method [2, 4.2.2] is used to implement the speed limit in the traffic dynamics. The activity of the speed limit is prescribed to be effective upon an interval I of length L_{res} centered at the position $x = 2000m$. The velocity represented by the speed limit is u_{lim}. Within the interval I the dynamics are prescribed so that drivers travelling at a speed greater than u_{lim} will brake so that their speed will be decreased to match the speed limit. The values can be found in Table 3.1. In the area where the speed limit applies there is the following modification to the braking force term:

$$B = \min\{c_1 \left(\frac{\rho_{max}\rho^+}{\rho_{max} - \rho^+} \right) (u - u^{lim}), F\} \text{ if } x \in I \text{ and } u > u_{lim}.$$

Aside from this modification the model remains otherwise unchanged. To initialize the simulation, constant densities in the range of $10\% - 40\%$ of the maximal density were applied, along with the associated constant velocities $U^e(\rho)$ derived using the fundamental diagram. As ever, the resultant wave patterns are studied.

The solution is presented in Figures (3.7) and (3.8) for the fundamental diagrams (3.12) and (3.13), respectively. In both Figures (3.7) and (3.8) two reaction times ($\tau = 0$ and $\tau = \frac{1}{4}$) are shown (in the top and bottom rows, respectively). Red dots indicate the area where the speed limit is applied. The differences in shape between the two fundamental diagrams considered give rise to differences in the resulting initial velocity profiles. As a result the braking patterns in Figure (3.8) are more pronounced. As before, step-like features are observed in the speed profiles, in conjunction with high oscillations in the density evolution.

In Figure (3.8) associated with fundamental diagram (3.13), for the high initial-density solution (green) with reaction time $\tau = 0$ (top row), density reached the maximal density at time $T^* \simeq 6.70s$. For the simulation with reaction time $\tau = \frac{1}{4}$ (bottom row), density also reached the maximal density: in this case, for the intermediate initial-density solution (black) at time $T^* \simeq 1.49s$. Reaching the maximal density means that a collision has occurred, and that the simulation should not be continue as, after a collision the model is no longer applicable. Thus in Figure (3.8), in the simulation for the high initial-density solution (green) with $\tau = 0$ (top row), and the intermediate initial-density solution (black) with $\tau = \frac{1}{4}$ (bottom row), the interpretation is that the model is invalid beyond the time T^*. Figure (3.8) shows the simulations ending at $T^* \simeq 6.70s$ (top row) and $T^* \simeq 1.49s$ (bottom row) respectively.

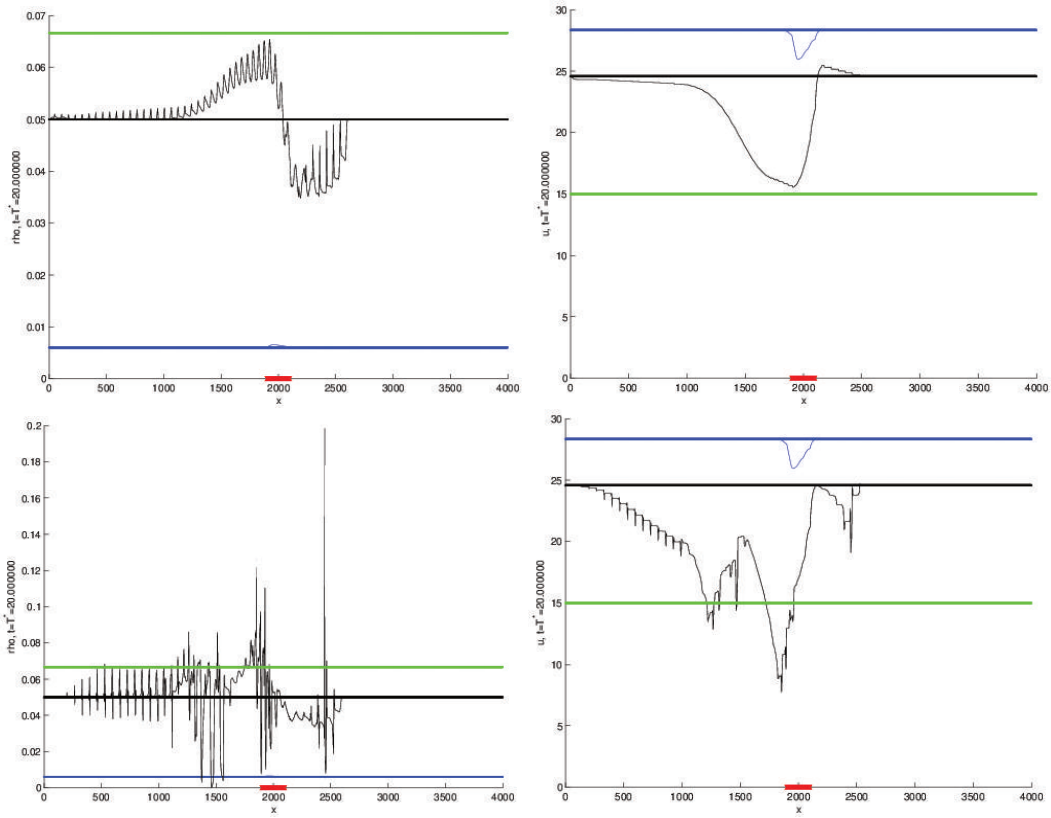

Figure 3.7: Density and velocity at time $T_{\max}$. Different initial densities correspond to different colors: blue (light traffic), black (intermediate traffic), green (moderately dense traffic). The speed limit u_{lim} is imposed within the red area. Fundamental diagram (3.12) and reaction times $\tau = 0$, $\tau = \frac{1}{4}$ were used in the simulations. Left: density, right: velocity.

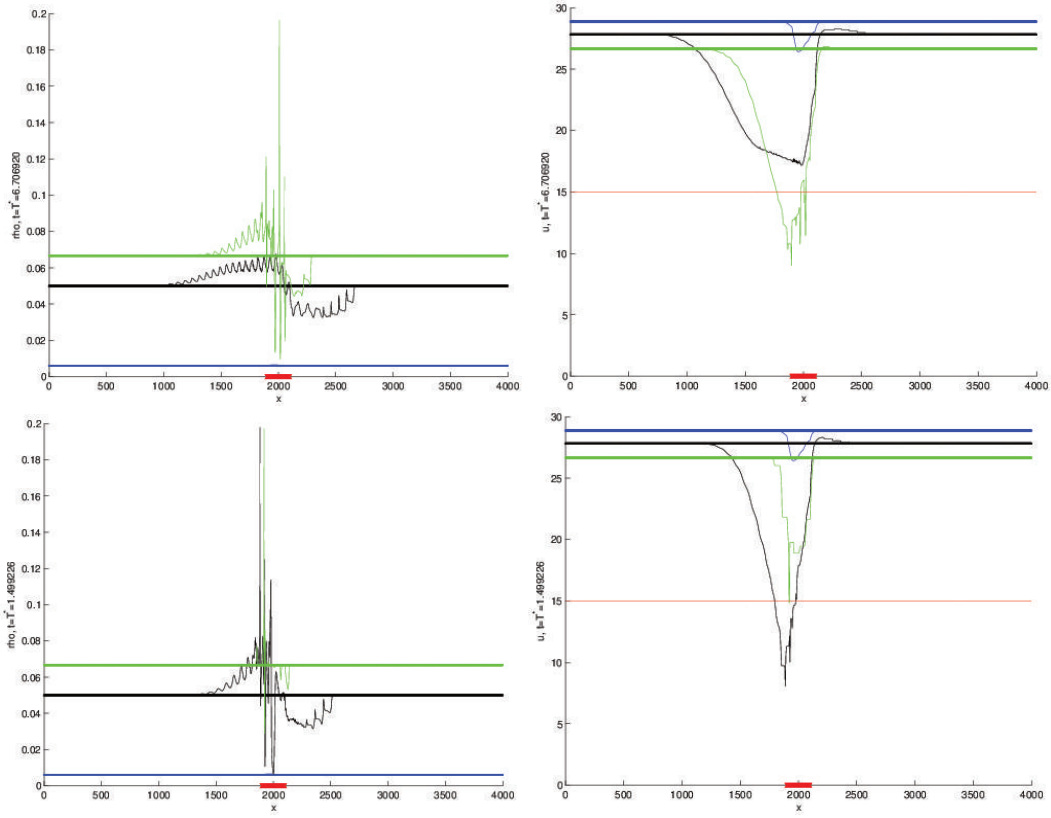

Figure 3.8: Density and velocity at time $T^* \simeq 6.70s$ (top row) and $T^* \simeq 1.49s$ (bottom row). Different initial densities correspond to different colors: blue (light traffic), black (intermediate traffic), green (moderately dense traffic). The speed limit u_{lim} is imposed within the red area. Fundamental diagram (3.13) and reaction times $\tau = 0$, $\tau = \frac{1}{4}$ were used in the simulations. Left: density, right: velocity.

Chapter 4

Discussion

Here we summarize the accomplishments of the thesis, touching on some of the strengths and weaknesses.

In the first chapter macroscopic traffic models were introduced (with reference to microscopic and kinetic models) leading ultimately to the presentation (1.20) of the Herty-Illner macroscopic model [1, 2, 3, 9] – a model closely related to that of Aw-Rascle-Zhang [4, 5]. The Herty-Illner macroscopic model (1.20) was arrived at from the (Kinetic) Herty-Illner Vlasov model (1.14) of [20, 1, 3] by means of introducing the appropriate weak-solution concept (1.19).

Subsequently the relationship between the Herty-Illner macroscopic model (1.20) and that of Aw-Rascle-Zhang was shown (1.3.2) by simplification (in the case $\tau = 0$) of the Herty-Illner system via truncation of the Taylor series (1.40,1.41,1.42) for terms involving the non-local "forward speed" u^X (1.33) leading to an equation (1.43) of Hamilton-Jacobi type (with diffusion): this "truncated" model (1.43) was shown (1.3.2) to generalize the popular model of Aw-Rascle-Zhang [4, 5]. Furthermore the "truncated model" was generalized in the related form (1.53,1.54) including also the reaction time parameter τ: (1.53,1.54) were studied quantitatively (1.5) and qualitatively (1.5).

Several basic analytic properties were presented for the Aw-Rascle-Zhang macroscopic model (1.1.4) [4, 5] and the Herty-Illner macroscopic model (1.20) including a detailed treatment of the existence of weak solutions (1.19) for the (Kinetic) Herty-Illner Vlasov model (1.14), as well as justification (1.2.5) for some possible choices of force term for the macroscopic model (1.20). For (1.20) the travelling wave hypothesis (1.45) was used in the braking and acceleration cases to respectively derive two

iterated-functional-differential equations: the jam (1.50) and un-jam (1.52) equations.

Strengthening the underpinning of the analysis of wave solutions for the "truncated" ("localized") model [1] according to (1.43), an added consistency check (1.4.6) showed agreement (in the case $\tau = 0$ only) between:

- (1.53,1.54): the result of abridging (1.50,1.52) by Taylor-series truncation, and
- (1.55,1.56): the result obtained (as in [1]) by using the same steps in reverse, that is: applying the Taylor-series truncation to (1.20) followed by applying the travelling-wave ansatz.

Thus two approaches produced (for $\tau = 0$) the same "truncated" system, of which the second order ordinary-differential-equations (1.55,1.56) are representative. Analogous to those ordinary-differential-equations used in [1] to study the phase-plane dynamics of travelling (braking) waves (1.55,1.56) their effective generalizations according to the forms (1.53,1.54) accomodate the new [2] reaction-time parameter τ.

Corresponding to (1.53,1.54) representing the (localized) travelling wave solutions to the model, the existence proof originally given in [1] for the "truncated" model (1.55,1.56) was naturally extended (1.5) to include τ, the reaction-time parameter [2] by using (1.53,1.54) instead. The inequalities guaranteeing existence were updated accordingly (1.70,1.71). In the proof more emphasis was placed on the acceleration aspect. For both the acceleration and braking cases, the parameters representative of the inequalities for existence were expressed in a way (1.69) making immediately apparent the dependency of the bounds (1.70,1.71) in terms of the travelling wave speed (V).

Numerical integrations for the updated ordinary differential equations cf. (1.53,1.54) representative of the (localized) travelling wave solutions were given (1.2,1.3,1.4) for several choices of the parameters τ and V. Moreover, failure of the existence theorem in the braking case was demonstrated, for travelling wave speeds (V) high enough to violate (1.71).

In the second chapter the functional equations resulting from insertion of a travelling wave ansatz into the Herty-Illner model were considered, as follows:

- the jam equation (1.50) associated with braking waves and,
- the un-jam equation (1.52) associated with acceleration waves.

A novelty of the thesis is the derivation of the simplified version (2.9) of the un-jam functional equation (1.52) associated with the acceleration case, a derivation complementary to that for the simplified form (2.10) corresponding to the braking case (1.50) that was studied in detail in [9]. Following this derivation of the simplified un-jam equation (2.9) was a discussion (2.3.2) of the existence question for both functional equations with respect to the simplified format (2.10,2.9). Despite substantial progress towards a solution [9] the existence question remains mysterious, beautiful, and open!

In the third chapter the Herty-Illner macroscopic traffic model was augmented by the incorporation of a relaxation term (3.12,3.13) representative of free-flow dynamics. This relaxation term was necessary in order for the model to be endowed with the type of self-excitatory behavior expected to be necessary for the emergence of features consistent with stop-and-go oscillations. Simulations of this refined version of the Herty-Illner model (3.14,3.15) were presented for several parameter choices (3.1) in the context of several realistic traffic scenarios, as follows:

- the evolution of a density blip (3.3.2) representative of density increase due to lane-changing,
- the effect of a lane reduction (3.3.3) and,
- the effect of a speed limit (3.3.4).

Ultimately, realistic stop-and-go waves were observed (3.5) in the simulations (3.3.3). The observed wavelengths were between 50m and 100m – such observations are consistent with those derived from empirical studies. Simulations were stopped in the event of a collision (3.8), as the refined Herty-Illner model (3.14,3.15) no longer has meaning at any time in the future of a collision event.

Some weaknesses in the developments, representing points that might be valuable to address in future work include:

- the drawbacks of the localized modeling [1] which remain apparent,
- the lack of formal solution for the non-local functional equations [9], and,
- the need for detailed comparison between: the predictions of stable regimes (via the parameters α, β) offered by the (localized) travelling-wave solution existence

theorem, and: empirical data on the evolution of moving jams (and moving acceleration waves).

The developments are lent considerable strength by the reconciliation (3.14,3.15) of the non-local forces characteristic of the Herty-Illner models with the relaxation term (3.12,3.13) representative of free-flow dynamics. Owing to this reconciliation is the observation of qualitatively reasonable stop-and-go oscillations (3.5,3.3.3). Thus a possible formal explanation for emergence of stop-and-go waves is provided, in terms of the tension between the desire to accelerate and the need to brake – better understanding this tension is the intention "driving" the developments here. Finally, the possibility – of obtaining, from "localized" wave existence results, "target" traffic conditions that are unfavourable for jam formation (for use in traffic control systems) – represents an important advantage conferred by the macroscopic approach. Again, corroborating this with information of empirical origin represents a valuable subject for future inquiry.

What if, **not** unlike phase-transitions in **s**tatistical physic**s**,
improvement is predicated
.....
upon i**n**c**r**easin**g**ly collectiv**e** .. awareness of .. "***stop***–
and– .....
.....
.....
.....
.....
.....
.....
....
....
....
....
.... -go" .....
....
....
....
....
.... pheno- ....
-mena? .....
.....
Does some threshol**d** level
of

awareness

predicate the critical re-evaluatio**n** of
.....patterned.....
.....
..... behavio-
ur ?

Bibliography

[1] M. Herty and R. Illner, "On stop-and-go waves in dense traffic," *Kinetic and Related Models*, vol. 1, no. 3, pp. 437–452, 2008.

[2] M. Herty and R. Illner, "Analytical and numerical investigations of refined macroscopic traffic flow models," *Kinetic and Related Models*, 2010.

[3] M. Herty and R. Illner, "Coupling of non-local driving behaviour with fundamental diagrams," *submitted*, 2012.

[4] A. Aw and M. Rascle, "Resurrection of "second order" models of traffic flow," *SIAM J. Appl. Math*, vol. 60, no. 3, pp. 916–938, 2000.

[5] H. M. Zhang, "A non-equilibrium traffic model devoid of gas-like behavior," *Transportation Research Part B: Methodological*, vol. 36, no. 3, pp. 275 – 290, 2002.

[6] J. Hale, *Theory of Functional Differential Equations*. Springer-Verlag, 1977.

[7] J. Hale and S. M. V. Lunel, *Introduction To Functional Differential Equations*. Springer-Verlag, 1977.

[8] S. S. Cheng and W. Li, *Analytic Solutions of Functional Equations*. World Scientific, 2008.

[9] R. Illner and G. McGregor, "On a functional-differential equation arising from a traffic flow model," *SIAM J. Appl. Math*, 2011.

[10] R. J. Leveque, "The dynamics of pressureless dust clouds and delta waves," *Journal of Hyperbolic Differential Equations*, vol. 1, no. 3, pp. 315–327, 2004.

[11] R. J. LeVeque, *Numerical Methods for Conservation Laws*. Birkhauser Verlag, Basel, 1992.

[12] R. J. LeVeque, *Finite Difference Methods for Ordinary and Partial Differential Equations*. Society for Industrial and Applied Mathematics, Philadelphia, 2007.

[13] M. R. Flynn, A. R. Kasimov, J.-C. Nave, R. R. Rosales, and B. Seibold, "Self-sustained nonlinear waves in traffic flow," *Phys. Rev. E*, vol. 79, p. 056113, May 2009.

[14] B. Kerner and S. Klenov, "A microscopic model for phase transitions in traffic flow," *J. Phys. A: Math. Gen.*, vol. 31, pp. L31–L43, 2002.

[15] R. Illner, S. Bohun, S. McCollum, and T. van Roode, *Mathematical modelling: a case studies approach*. American Mathematical Society, 2005.

[16] R. Illner, C. Kirchner, and R. Pinnau, "A derivation of the aw-rascle traffic models from fokker-planck type kinetic models," *Quart. Appl. Math.*, no. 67, pp. 39–45, 2009.

[17] A. Klar, R. Kuehne, and R. Wegener, "Mathematical models for vehicular traffic," 1996.

[18] A. Klar and R. Wegener, "A hierarchy of models for multilane vehicular traffic i: Modeling," *SIAM J. Appl. Math*, vol. 59, no. 3, pp. 983–1001, 1998.

[19] A. Klar and R. Wegener, "A hierarchy of models for multilane vehicular traffic ii: Numerical investigations," *SIAM J. Appl. Math*, vol. 59, no. 3, pp. 1002–1011, 1998.

[20] R. Illner, A. Klar, and T. Materne, "Vlasov-fokker-planck models for multilane traffic flow," *Comm. Math. Sci.*, vol. 1, no. 1, pp. 1–12, 2003.

[21] A. Martial, R. Illner, and A. Richardson, "Analysis and simulations of a refined flocking and swarming model of cucker-smale type," *Kinetic and Related Models*, 2011.

[22] M. Günther, A. Klar, T. Materne, and R. Wegener, "An explicitly solvable kinetic model for vehicular traffic and associated macroscopic equations," *Mathematical And Computer Modelling*, vol. 2002, no. 35, pp. 591 – 606, 2002.

[23] D. Helbing, "Gas-kinetic derivation of navier-stokes-like traffic equations," *Phys. Rev. E*, vol. 53, pp. 2366–2381, Mar 1996.

[24] A. Aw, A. Klar, T. Materne, and M. Rascle, "Derivation of continuum traffic flow models from microscopic follow-the-leader models," *SIAM J. Appl. Math*, vol. 63, no. 1, pp. 259–278, 2002.

[25] R. Colombo, F. Marcellini, and M. Rascle, "A 2-phase traffic model based on a speed bound," *SIAM J. Appl. Math*, vol. 70, no. 7, pp. 2652–2666, 2010.

[26] J. Greenberg, A. Klar, and M. Rascle, "Congestion on multilane highways," *SIAM J. Appl. Math*, vol. 63, no. 3, pp. 818–833, 2003.

[27] R. Wegener and A. Klar, "A kinetic model for vehicular traffic derived from a stochastic microscopic model," *Transport Theory and Statistical Physics*, vol. 25, pp. 79–8, 1996.

[28] M. J. Lighthill and G. B. Whitham, "On kinematic waves.," *Proceedings of the Royal Society of London. Series A, Mathematical and Physical Sciences*, vol. 229, no. 1178, pp. 281–345, 1955.

[29] P. I. Richards, "Shock waves on the highway," *Operations Research*, vol. 4, no. 1, pp. 42–51, 1956.

[30] G. Whitham, *Linear And Nonlinear Waves*. John Wiley And Sons, 1974.

[31] C. F. Daganzo, "Requiem for second-order fluid approximations of traffic flow," *Transportation Research Part B: Methodological*, vol. 29, no. 4, pp. 277 – 286, 1995.

[32] M. Kuczma, *An introduction to the theory of functional equations and inequalities: Cauchy's equation and Jensen's inequality*. Birkhuser, Basel, 2009.

[33] O. Diekmann, S. A. van Gils, S. M. Lunel, and H.-O. Walther, *Delay equations: functional-, complex-, and nonlinear analysis*. Springer-Verlag, 1996.

[34] J. Wu, *Theory and applications of partial functional differential equations*. Springer-Verlag, 1996.

[35] H. Zhao, "Analytic solutions for a functional differential equation related to a traffic flow model," *submitted*, 2012.

[36] M. E. M. Kimathi, *Mathematical Models for 3-Phase Traffic Flow Theory.* PhD thesis, Kaiserslautern, 2012.

[37] J. Greenberg, "Traffic congestion – an instability in a hyperbolic system," *Bulletin of the Institute of Mathematics, Academica Sinica (New Series)*, vol. 2, pp. 123–138.

[38] B. Kerner, *The Physics of Traffic.* Springer, Berlin, 2004.

[39] M. Herty, R. Illner, A. Klar, and V. Panferov, "Qualitative properties of solutions to systems of fokker-planck equations for multilane traffic flow.," *Transp. Theory Stat. Phys.*, vol. 35, pp. 31–54, 2006.

[40] G. M. Coclite, M. Garavello, and B. Piccoli, "Traffic flow on a road network," *SIAM J. Math. Anal.*, vol. 36, pp. 1862–1886, 2005.

[41] J. Greenberg, "Extensions and amplifications of a traffic model of aw and rascle.," *SIAM J. Appl. Math.*, vol. 62, pp. 729–745, 2001.

[42] J. Greenberg, "Congestion redux," *SIAM J. Appl. Math.*, vol. 64, pp. 1175–1185, 2004.

[43] M. Herty and A. Klar, "Modelling, simulation and optimization of traffic flow networks," *SIAM J. Sci. Comp.*, vol. 25, pp. 1066–1087, 2003.

[44] J. P. Lebacque, "Les modèles macroscopiques de traffic," *Annales des Ponts 67*, vol. 3, pp. 28–45, 1993.

[45] R. Herman and I. Prigogine, "A two-fluid approach to twon traffic," *Science*, vol. 204, pp. 148–151, 1979.

[46] M. Herty and M. Rascle, "Coupling conditions for a class of second-order models for traffic flow," *SIAM J. Math. Anal.*, vol. 38, pp. 595–616, 2006.

[47] I. Gasser, T. Seidel, G. Sirito, and B. Werner, "Bifurcation analysis of a class of car following traffic models ii: Variable reaction times and agressive drivers," *Bulletin of the Institute of Mathematics, Academica Sinica (New Series)*, vol. 2, pp. 587–607, 2007.

[48] I. Gasser, G. Sirito, and B. Werner, "Bifurcation analysis of a class of 'car following' traffic models," *Physica D*, vol. 197, pp. 222–241, 2004.

[49] D. Helbing, *Traffic dynamics. New physical concepts of modelling.* Springer, Berlin, 1997.

[50] D. Helbing, A. Hennecke, V. Shvetsov, and M. Treiber, "Micro- and macro-simulation of freeway traffic.," *Math. Comput. Modelling*, vol. 35, pp. 517–547, 2002.

[51] M. Treiber and D. Helbing, "Macroscopic simulation of widely scattered synchronized traffic states.," *J. Phys. A, Math. Gen.*, 1999.

[52] L. Santen, A. Schadschneider, and M. Schreckenberg, "Towards a realistic microscopic description of highway traffic," *J. Phys A*, vol. 33, pp. 477–485, 2000.

[53] S. Marinosson, R. Chrobok, A. Pottmeier, J. Wahle, and M. Schreckenberg, *Cellular Automata*, vol. 2493 of *Lecture Notes in Comput. Sci.*, ch. Simulation framework for the autobahn traffic in North Rhine-Westphalia, pp. 315–324. Springer, Berlin, 2002.

[54] E. Ben-Naim, P. L. Krapinsky, and S. Redner, "Kinetics of clustering in traffic flows," *Physical Rev. E*, vol. 50, pp. 822–829, 1994.

[55] T. Alperovich and A. Sopasakis, "Stochastic description of traffic flow," *J. Stat. Phys.*, vol. 133, pp. 1083–1105, 2008.

[56] A. Sopasakis and M. A. Katsoulakis, "Stochastic modeling and simulation of traffic flow: Asymmetric single exclusion process with arrhenius look-ahead dynamics," *SIAM J. Appl. Math*, vol. 66, no. 3, pp. 921–944, 2006.

[57] A. Chertock, A. Kurganov, and Y. Rykov, "A new sticky particle method for pressureless gas dynamics," *SIAM J. Numer. Anal.*, vol. 45, pp. 2408–2441, 2007.